

# A Framework for construction of and computations on Four-Dimensional Aircraft Trajectories

CMSC 663-664

2016-2017

**Author:**

**Jon Dehn**

[jondehn@umd.edu](mailto:jondehn@umd.edu)

**Advisor:**

**Dr. Sergio Torres**

**Fellow, Leidos Corporation**

[Sergio.torres@leidos.com](mailto:Sergio.torres@leidos.com)

**Final Report – May 12, 2017**

# Abstract

Air traffic control systems perform many functions in order to safely and efficiently move air traffic through the national and international airspace. A key component of these systems is an accurate prediction of where the individual flights will be over time. This project builds a framework to both do that prediction and use the prediction to examine various air traffic control algorithms for both accuracy and efficiency. This framework is designed for reuse, such that future research into ATC algorithms can be conducted with simple extensions to the system.

## Table of Contents

1	Introduction .....	6
2	Project Goal.....	6
3	Approach.....	7
4	Scientific Computing Algorithms.....	8
4.1	Background Concepts .....	8
4.1.1	Coordinate system .....	8
4.1.2	Speed Definitions .....	8
4.2	Trajectory Generation.....	9
4.2.1	Trajectory Generation Basics – latitude and longitude dimension.....	9
4.2.2	Trajectory generation basics – altitude and time .....	10
4.2.3	Rate of Climb/Descent .....	11
4.2.4	Trajectory Generation Inputs.....	14
4.2.5	Trajectory Generation Details .....	15
4.3	Use of Weather Forecast Models .....	16
4.4	Wind Optimal Trajectories.....	17
4.4.1	Version 1 .....	18
4.4.2	Version 2 .....	20
4.5	Parallelizing Conflict Detection .....	21
4.5.1	Time Filter .....	23
4.5.2	Horizontal Filter .....	24
4.5.3	Parallelization Strategies.....	27
5	Implementation .....	31
6	Validation Methods.....	31
7	Test Problems for Verification .....	33
7.1	Use of Weather Forecast Models .....	33
7.2	Wind Optimal Trajectories.....	33
7.3	Parallelizing Conflict Detection .....	33
8	Results.....	34
8.1	Use of Weather Forecasts.....	34
8.1.1	Quality of Forecast .....	34
8.1.2	Impact on Flight Time .....	35
8.2	Wind Optimal Trajectories.....	37

8.3	Parallel Processing .....	37
9	Conclusion.....	40
Appendix A.	Timeline.....	40
Appendix B.	Milestones.....	40
Appendix C.	Deliverables.....	41
Appendix D.	Bibliography .....	41
Appendix E.	List of Abbreviations .....	41

## List of Figures

Figure 1 Framework Design .....	7
Figure 2 Horizontal path for sample flight .....	10
Figure 3 Vertical profile of sample flight.....	11
Figure 4 Lambert vs. Spherical grids .....	15
Figure 5 Flights Paths for the Use of Forecasted Weather analysis.....	17
Figure 6 Wind Optimal Trajectories, Version 1 .....	19
Figure 7 Wind Optimal Trajectories, Version 2 .....	21
Figure 8 Conflict Detection Time Filter .....	23
Figure 9 Conflict Detection Altitude Filter .....	23
Figure 10 Conflict Detection Horizontal Filter - part 1.....	24
Figure 11 Conflict Detection Horizontal Filter - part 2.....	25
Figure 12 Conflict Detection Horizontal Filter - part 3.....	25
Figure 13 Conflict Detection Horizontal Filter - part 4.....	26
Figure 14 Conflict Detection Horizontal Filter - part 5.....	26
Figure 15 Conflict Detection Horizontal Filter - part 6.....	27
Figure 16 NVIDIA CPU/GPU Architecture.....	28
Figure 17 Memory moves for strategy 2 .....	29
Figure 18 Memory moves for strategy 3 .....	30
Figure 19 Trajectory Generation Comparison .....	32
Figure 20 Effect of Wind on Trajectories .....	33
Figure 21 Test flights used for Conflict Detection.....	34
Figure 22 Accuracy of Forecasted Wind Speed.....	35
Figure 23 Distribution of flight time differences with forecasted weather .....	36
Figure 24 Summary of Flight Time Errors .....	37

## 1 Introduction

Global Air Traffic Control (ATC) is distributed among multiple Flight Information Regions (FIRs). Each country is responsible for safely and efficiently handling traffic in their FIRs. Most countries have 1 FIR; due to the volume of air traffic and the complexity of its airspace, the US has 20.

At the core of the FIR's processing is building an estimate of each aircraft's *trajectory* (a four dimensional description of the flight path, with dimensions of latitude, longitude, altitude and time).

Once these trajectories are constructed, they are used for various purposes, such as *conflict detection* (which predicts whether two aircraft will be too close to each other, or if a single aircraft will fly into restricted airspace), workload planning for the human controllers separating air traffic, airport arrival and departure planning, etc.

This project examines different aspects of generating and using these trajectories, including performance aspects of using the trajectories in various applications.

## 2 Project Goal

The project has built a modular system where:

1. Different trajectory generation algorithms can be tested
2. Algorithms using those trajectories can be tested for performance and accuracy. The specific algorithms selected have relevance to the state of the practice today.

This framework can be used to explore new concepts for air traffic management.

A secondary goal is that the project's author becomes familiar with techniques of parallelizing computing algorithms, and becomes more proficient in the use of the Python programming language.

### 3 Approach

The system looks like this:

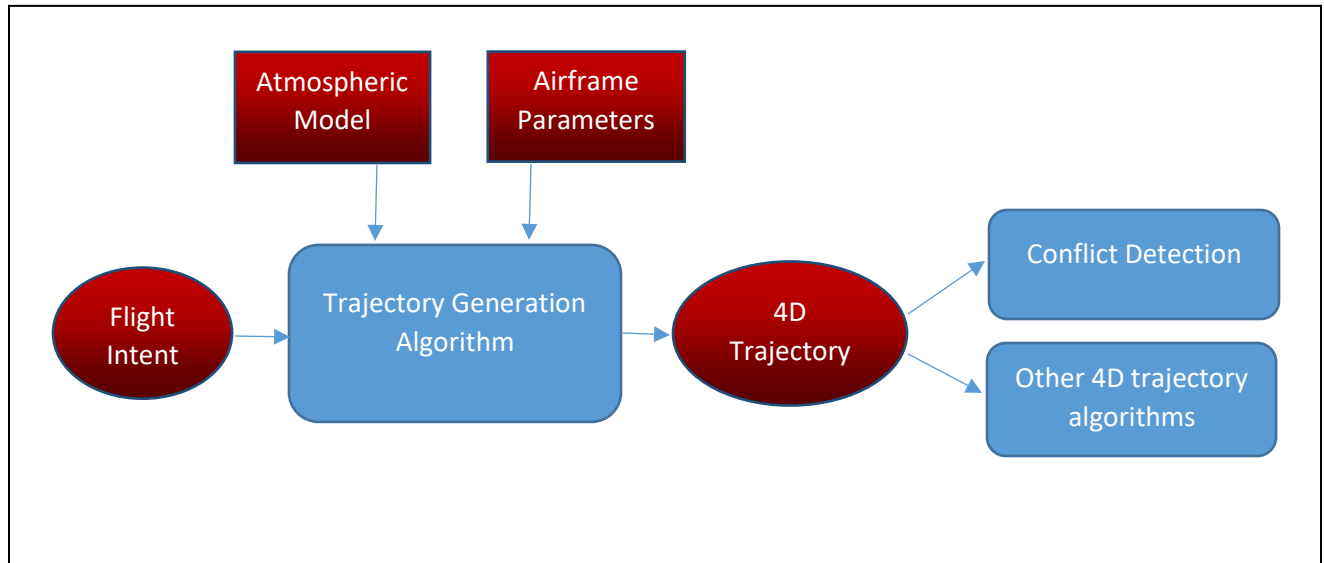


Figure 1 Framework Design

The trajectory generation algorithm takes three major inputs:

- 1) Flight intent, consisting of items such as route of flight, departure time, desired airspeed, type of aircraft and desired cruising altitude  
Flight Intent can be either synthetic for testing or derived from real-world data (via the publicly available “Aircraft Situation Display to Industry” (ASDI) data stream, or websites such as “FlightAware”[9]).
- 2) An atmospheric model, listing temperatures, pressures and wind aloft values for the FIR’s geographic region. One instance of this is a three-dimensional model, but multiple hour forecasts are available, which adds a fourth dimension. This is publicly available from NOAA, and are distributed in “GRIB2” format[6]. These files typically use a Lambert conical projection, which would be transformed into a grid of fixed sized cells, with fixed sized latitude, longitude and altitude[8].  
Initial testing can be done with a “null” model of zero winds.
- 3) A set of airframe parameters, that indicate how particular aircraft types (such as a Boeing 737) will climb and descend. For this, Eurocontrol’s Base of Aircraft Data (BADA) dataset[1] is used (under the University of Maryland license). There are two versions of this model in use; version 3 (which has a rich set of airframe parameters) and version 4 (which is more detailed but covers fewer airframes currently). This project uses version 3.

These experiments were proposed; time constraints precluded completing the final experiment. The first three were completed, and are discussed in this report.

- 1) The current US system uses current-hour weather model for all computations, even though a flight can last several hours. Implement a version that uses future weather forecasts and compare changes in long-duration trajectories
- 2) Find an optimal wind-aided trajectory. This will find an “optimal” trajectory between two points given non-zero wind patterns. Initially, “optimal” will be define as the trajectory that uses the least fuel; other more complex definitions could be supplied.
- 3) Parallelize conflict detection algorithms, measure complexity of implementation vs. speed tradeoffs for different parallel techniques
- 4) Look at the increased accuracy of BADA version 3 vs. version 4 for identical aircraft types, balanced against the increase in complexity and computational load

The algorithms for each experiment are described in the next section.

## 4 Scientific Computing Algorithms

The principal algorithm that is implemented is the generation of the 4D trajectory; this requires the solution of the ordinary differential equation to describe the climb and descent segments of the trajectory. Some basic concepts are discussed first.

### 4.1 Background Concepts

#### 4.1.1 Coordinate system

Points on the earth’s surface are transformed to a Cartesian coordinate  $(x,y,z)$  on a unit sphere (radius = 1.0). Given the radius of the earth, distances on the surface of the unit sphere are converted to nautical miles (NMI), for things like speed calculations (Knots). Other calculations such as intersection of great circle arcs are simplified when the unit sphere is used.

Since we are concerned with a particular geographic area, an approximation of the earth’s radius for that area would be used in practice (perhaps slightly different for each FIR). For this project, the mean radius of the earth will be used.

All external latitude/longitudes are supplied in WGS 84 coordinates[2], which assumes the earth is an ellipsoid with specific major and minor axes (same as is used by the GPS). Translation to the unit sphere is straight forward, and supplied as routines in many programming languages.

Note that the Cartesian coordinate  $(x/y/z)$  is for the surface of the earth. Altitude above the surface is separately specified (and forms one dimension of each trajectory point). This simplifies the ODE to be solved, since it depends on altitude, not distance from the earth’s center.

#### 4.1.2 Speed Definitions

The algorithms use several different “speed” values, as described below.

**True Airspeed (TAS)** – speed of the aircraft relative to the surrounding air mass (which may be moving with respect to the earth’s surface)



**Ground speed** – speed of the aircraft over the surface of the earth; this is the true airspeed adjusted by the winds moving the air mass. If wind speed and TAS are given as vectors,  $V_{GS} = V_{TAS} + V_{WIND}$ .

**Calibrated airspeed (CAS)** – airspeed as known to the aircraft’s instrumentation; this is based on a “calibration” that takes into account any known bias in the instruments. For a constant CAS, TAS will vary depending on altitude

**Mach** – speed of sound; important here because aircraft plan to hold CAS and Mach constant; there is a *crossover altitude* at above which planning is done based on Mach speed, CAS and Mach will be equal at that altitude.

## 4.2 Trajectory Generation

### 4.2.1 Trajectory Generation Basics – latitude and longitude dimension

As noted above, the trajectory generator takes flight intent as an input. This is supplied by the airline or pilot, and consists of:

- The path (over the surface of the earth) to be followed
- The desired cruise altitude
- The desired cruise speed (true airspeed or Mach; in practice only military flights specify this in Mach)
- The type of airplane (e.g. Boeing 737)
- Departure time

As an example, consider Southwest flight 3156 from Baltimore (airport code BWI) to Orlando (MCO):

- altitude 40,000 feet
- speed 452 knots
- Boeing 737-300
- Depart at 10:35 am

The creation of the actual path from departure airport to destination airport is beyond the scope of this project; we start with the expanded set of points as an input. This input defines a path on the earth’s surface, which starts at the departure airport, ends at the destination airport, and has intermediate *waypoints*. The waypoints are connected by great circle arcs. In order to more accurately follow the path of the flight, turn waypoints can be replaced with a number of smaller segments that more closely approximate the turn to be taken. Whether this is done depends on the accuracy needed for other work. Figure 2 shows an example path from Baltimore to Orlando.

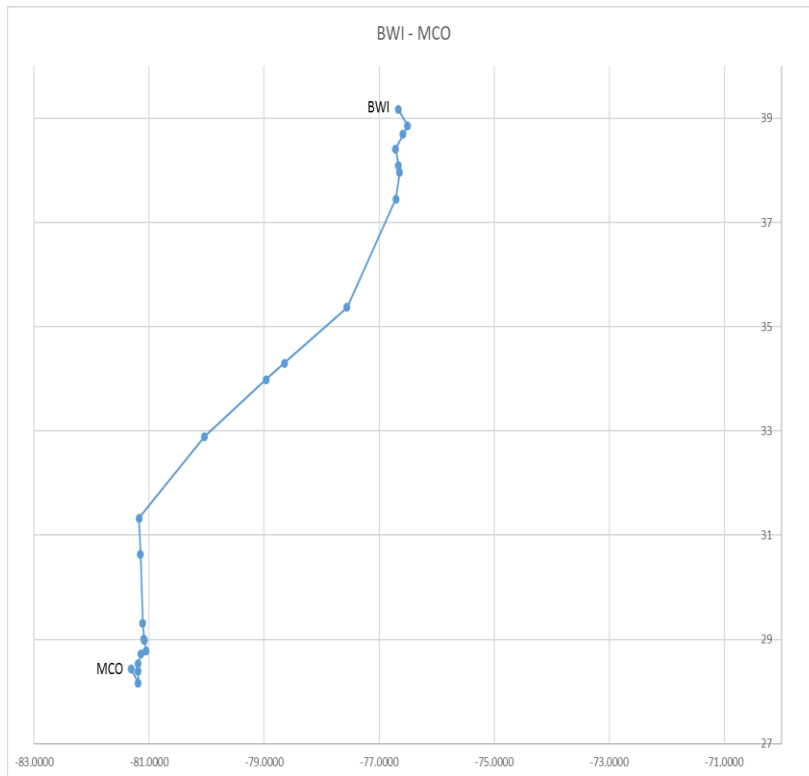


*Figure 2 Horizontal path for sample flight*

#### 4.2.2 Trajectory generation basics – altitude and time

In order to turn the two-dimensional waypoints into points on a four-dimensional trajectory, altitude and time are calculated for each point. This results in a vertical profile that looks something like Figure 3.

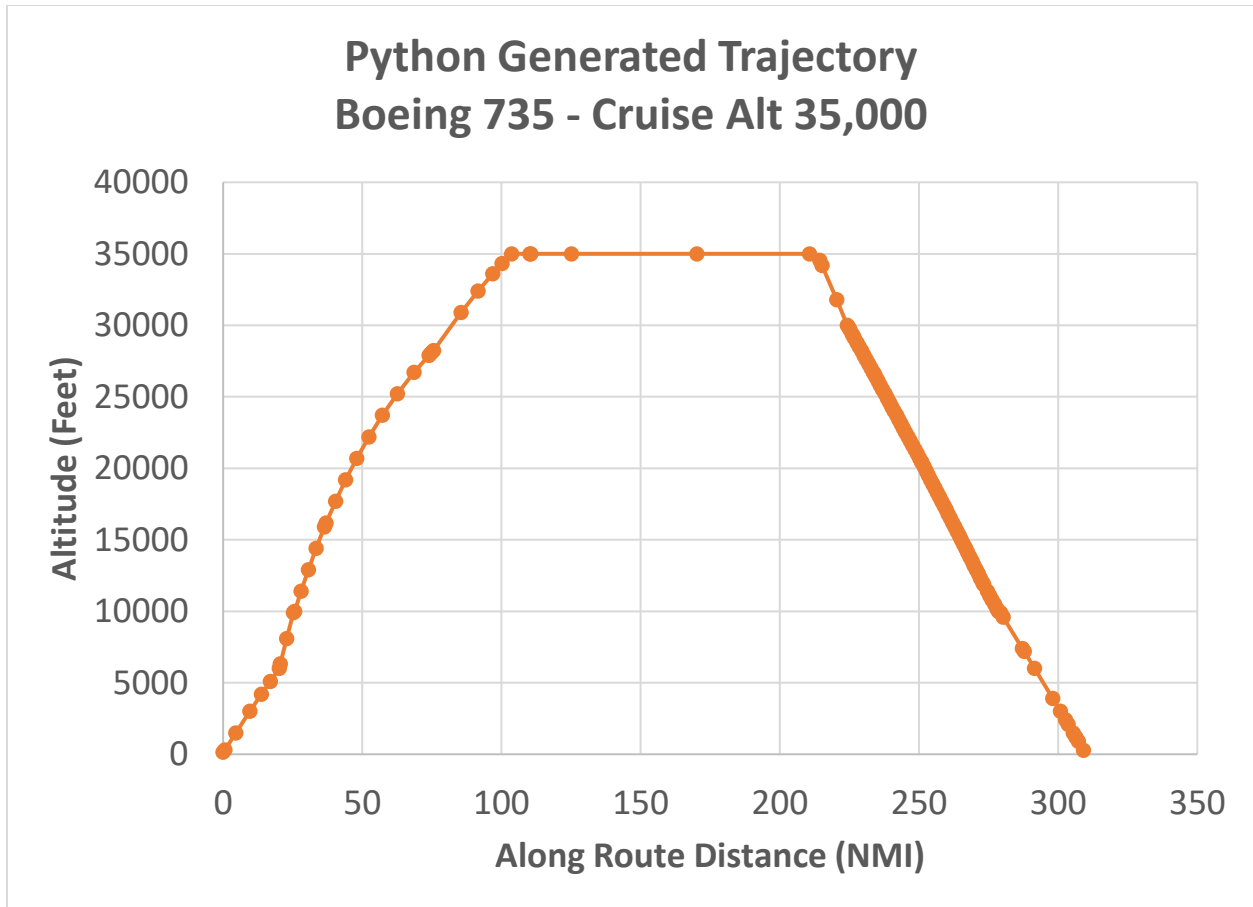


Figure 3 Vertical profile of sample flight

Each trajectory point is called a *cusps*, and the segments that connect cusps have a constant rate of vertical velocity (climb or descent) and a constant rate of acceleration over the segment. This, along with the starting ground speed for each segment, allows us to predict where a flight will be at any point in time.

This final representation of the trajectory has additional points added between the waypoints supplied as inputs, in order to assure that the above definition of constant acceleration/vertical velocity holds. For example, it is necessary to accelerate to the desired climb speed; when that acceleration is complete a cusp is added to the trajectory.

#### 4.2.3 Rate of Climb/Descent

Calculation of the rate of climb (or descent) is described in detail in [1], and is summarized here.

The basis of this rate is this conservation of energy equation:

$$(\text{Thr} - D) * V_{\text{TAS}} = mg_0 \frac{dh}{dt} + mV_{\text{TAS}} \frac{dV_{\text{TAS}}}{dt} \quad (4.2.3 - 1)$$

Where

<b>Thr</b>	Thrust supplied by the aircraft engines	<b>m (mass)</b>	Mass of the aircraft, including fuel, passengers and baggage. This will decrease over the life of the flight
<b>D (Drag)</b>	Drag from movement through the atmosphere	<b>g<sub>0</sub></b>	Gravitational acceleration
<b>V<sub>TAS</sub></b>	Velocity in true airspeed	<b>h</b>	Geodetic altitude

Combine this equation with the assumption that, during climbs and descents, pilots hold speed (CAS or Mach) and throttle position constant, the above can be re-written as

$$\frac{dh}{dt} = \frac{(\text{Thr} - D) * V_{TAS}}{mg_0} \left[ 1 + \left( \frac{V_{TAS}}{g_0} \right) \left( \frac{dV_{TAS}}{dh} \right) \right]^{-1} \quad (4.2.3 - 2)$$

The last term can be replaced by an “energy share factor” [3]; the ratio of energy allocated to climb vs. acceleration for a constant velocity; a function of Mach:

$$f\{M\} = \left[ 1 + \left( \frac{V_{TAS}}{g_0} \right) \left( \frac{dV_{TAS}}{dh} \right) \right]^{-1} \quad (4.2.3 - 3)$$

Hence, the rate of climb or descent (which is typically expressed in pressure altitude H<sub>p</sub>, rather than geodetic altitude h), is

$$ROCD = \frac{dH_p}{dt} = \frac{T - \Delta T}{T} \left[ \frac{(\text{Thr} - D) * V_{TAS}}{mg_0} \right] f\{M\} \quad (4.2.3 - 4)$$

Where T is temperature at altitude, and ΔT is the temperature differential at that altitude from the International Standard Atmosphere (this is given by the atmospheric model).

#### 4.2.3.1 Energy Share Factor

The energy share factor  $f\{M\}$  is a function of Mach (M) and varies with altitude, and whether we are accelerating or decelerating in climb or descent. As an example (to convey the complexity of the equation), below the crossover altitude when not accelerating, it is defined as:

$$f\{M\} = \left\{ 1 + \frac{\kappa R \beta_{T,<}}{2g_0} M^2 \frac{T - \Delta T}{T} + \left( 1 + \frac{\kappa - 1}{2} M^2 \right)^{\frac{-1}{\kappa - 1}} \left\{ \left( 1 + \frac{\kappa - 1}{2} M^2 \right)^{\frac{\kappa}{\kappa - 1}} \right\} - 1 \right\}^{-1} \quad (4.2.3 - 5)$$

Where

- κ**      Adiabatic index of air = 1.4
- R**      Real gas constant for air = 287.05287

$\beta_{T,<}$  ISA temperature gradient below the tropopause - -0.0065

The Mach number is based on the current speed at the current altitude, which may be a true airspeed. If so, that TAS is converted to a Mach value by dividing the  $V_{TAS}$  by the speed of sound at the given altitude (the value for T is obtained from the weather model at the current altitude):

$$M = \frac{V_{TAS}}{\sqrt{\kappa RT}} \quad (4.2.3 - 6)$$

The full definition of the energy share factor can be found in [1].

#### 4.2.3.2 Thrust

Thrust depends on the engine type (Jet, Turboprop or Propeller), pressure altitude, airspeed (in some cases) and temperature differential.

For example, for a jet engine, the maximum climb thrust would be:

$$(Thr_{max climb})_{ISA} = C_{TC,1} * \left( 1 - \frac{H_p}{C_{TC,2}} + C_{TC,3} * H_p^2 \right) \quad (4.2.3 - 7)$$

Where the coefficients  $C_x$  are given for the airframe type in the BADA dataset. Note that in this case (of a jet engine) there is no term for airspeed.

#### 4.2.3.3 Drag

Drag depends on the Drag Coefficient, which in turn depends on the lift coefficient.

Lift coefficient:

$$C_L = \frac{2 * m * g_0}{\rho * V_{TAS}^2 * S * \cos \emptyset} \quad (4.2.3 - 8)$$

Drag Coefficient:

$$C_D = C_{D0,CR} + C_{D2,CR} * (C_L)^2 \quad (4.2.3 - 9)$$

And finally drag force:

$$D = \frac{C_D * \rho * V_{TAS}^2 * S}{2} \quad (4.2.3 - 10)$$

- S** Wing surface area
- $\rho$**  Air density
- $\emptyset$**  Bank angle (zero, unless in a turn)

#### 4.2.3.4 *Weather Model*

The weather model supplies some key data for the above equations. Specifically, the following information is used from the NOAA-supplied data:

- 1) North wind component
- 2) East wind component
- 3) Temperature (from which the  $\Delta T$  can be calculated)
- 4) Pressure

#### 4.2.4 *Trajectory Generation Inputs*

##### 4.2.4.1 *Flight Intent Source*

The FlightAware web site ([www.flightaware.com](http://www.flightaware.com)) provides intent (airspeed, cruise altitude, route of flight, departure time) for all commercial flights in the US. Once a pair of endpoint airports is selected, that site provides the fixes in the route for a variety of flights between those cities. This data is screen-scraped (using a developed Python program) to produce an intent file that can be used in various experiments.

Flights of various durations and directions can therefore be added to the inventory of test data.

##### 4.2.4.2 *Airframe Parameters*

Eurocontrol's BADA database is used (by extending the University's existing license for use on this project); version 3.13 is the latest version as of fall 2016; it is used for this effort.

##### 4.2.4.3 *Atmospheric Model*

GRIB2 files, with atmospheric levels, are provided hourly by NOAA. Selected days data is captured and converted to a form usable by the program. That conversion follows this process:

- 1) The data from NOAA is provided in various resolutions; for this effort the 40 km grid is used, with the data covering the continental US.
- 2) That data is processed by NOAA's "degrib" tool [10] to produce ASCII files (in comma-separated-value format, CSV) containing:
  - a. Grid Coordinates (x/y)
  - b. Latitude and Longitude (in geodetic coordinates) of that grid point
  - c. Value for the parameter; the temperature, U wind value, V wind value and pressure values are used here
- 3) Data in the CSV file is in the Lambert Conical Projection, with a secant line of 25 degrees north latitude. When building a trajectory, fast access to weather data in a spherical (conformal) grid is needed. Hence the data is transformed to a lat/long grid in equally-spaced conformal latitude and longitude, in equally spaced altitude bands of 1000 feet. This data is then written to disk using the "numpy" Python package (which stores dense arrays of floating point data). During trajectory generation, the particular set of weather data and these files are read for use during processing. Numpy is used in various places in this project, but (at this point) only for its efficient in memory representation of large arrays, and the load and store operations on those arrays.

The transformation from Lambert to Spherical requires that a spherical grid be constructed that lies within the Lambert data. The values of each parameter at the spherical grid points is an interpolated

value from the Lambert grid. In the horizontal direction, a bi-linear interpolation is used from the four surrounding Lambert grid points; these horizontal points (which are at pressure levels 1000 mb through 100 mb) are then linearly interpolated in the vertical direction to give values at evenly spaced 1000 foot altitude bands. This is the same technique as is detailed in "ERAM Flight Data Processing (FDP) and Weather Data Processing (WDP) Algorithms" [8].

The grids are shown in Figure 4. This figure is shown with latitude distances unchanging with longitude (that is, no special projection). The **blue** Lambert grid appears to expand towards the north, since in fact the longitudinal spacing will decrease as we go north. The **red** spherical grid that is created by the program is designed to fit completely in inside the Lambert grid, so that only interpolation is needed to find point values. The **green** box shows the extent of the lower 48 states; the part that is outside the red grid to the east is the eastern-most tip of Maine. If this setup modeled a flight in that remote part of Maine, no wind or temperature information would be available.

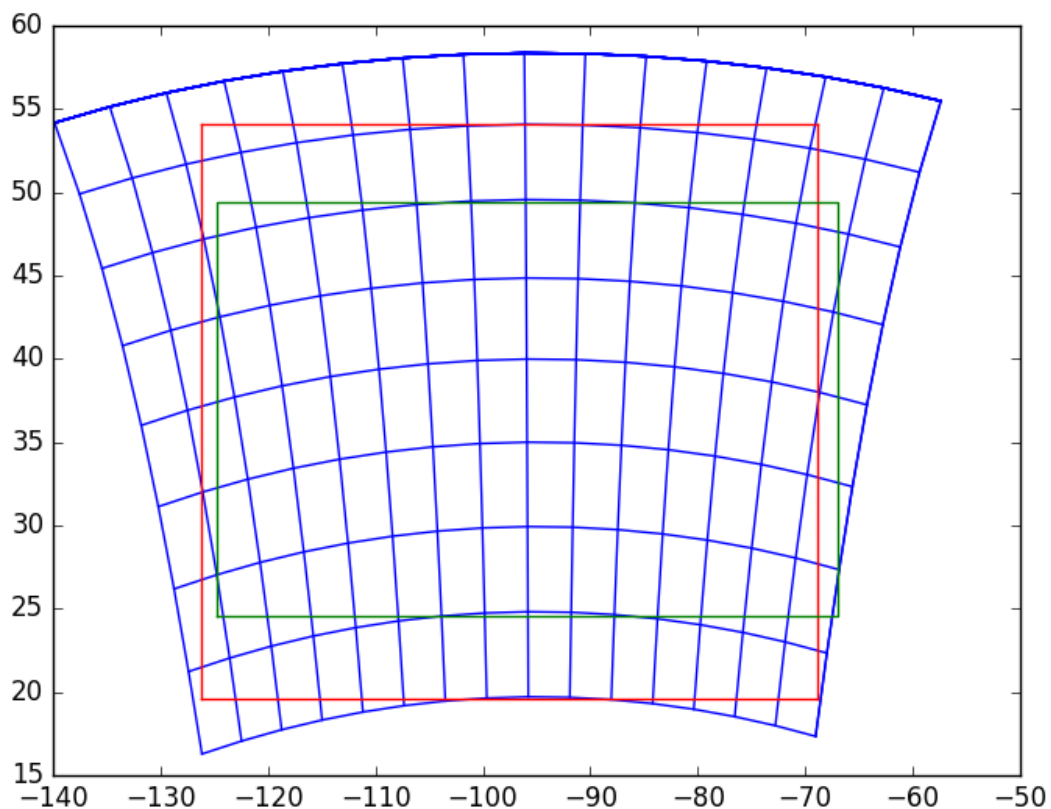


Figure 4 Lambert vs. Spherical grids

#### 4.2.5 Trajectory Generation Details

Using the above definitions, the ordinary differential equation given for ROCD (Equation 4.5-4) is solved using a Runge-Kutta technique (Python provides some existing code in this area, `scipy.integrate.ode` provides Runge-Kutta solutions for order 4 and 8 with configurable step size). This describes the climb or descent phases; the cruise phase (moving at constant true airspeed) is simply following the route of

flight from one waypoint to another. Note that the time associated with each cusp is calculated from the ground speed and ground speed acceleration applied to get from one cusp to the other. Ground speed is derived from the true airspeed by applying the wind observed at the altitude of the cusp.

While the descent phase also involves solving the ODE for ROCD, there is one additional complication; that equation requires mass to be known at each cusp. In this case, we know where we want to end (the destination airport), but the point at which to start the descent is not precisely known. An iterative technique is used:

- 1) First, make a gross approximation of the top of descent point.
- 2) Solve the ODE, descending to the destination airport's altitude.
- 3) If we are within a small epsilon of the airport, the iterations are done. The choice of epsilon affects how many iterations are necessary; in this case, an epsilon of approximately 1000 feet (shorter than commercial airport runways) is appropriate.
- 4) Otherwise, move the top of descent point forward or backward along the route defined by the waypoints, in order to get closer to the destination airport, and repeat starting at step 2.

The movement of the top of descent point can be summarized as follows:

- 1) Let  $TOD_k$  represent the top of descent point for iteration "k". This is measured in distance along the route from the departure airport. This is termed the "along route distance", or ARD.
- 2) Let AP represent the ARD of the destination airport; this is the known distance at the end of the trajectory
- 3) On any iteration k, the ARD when the trajectory is modeled to reach the destination airport is denoted as  $D_k$ .
- 4) Let function E, at any iteration k, represent the difference between the actual outcome ( $D_k$ ) and the desired outcome (AP). When this function is zero, we are done. So  $E_k = (D_k - AP)$ .
- 5) The algorithm becomes:
  - a. Take an initial guess at  $TOD_0$ ; this will be based on some standard descent rate.
  - b. Calculate  $D_0$ .
  - c. Set  $TOD_1 = TOD_0 - E_0$
  - d. Compute  $E_k$  (initially for  $k=1$ )
  - e. If  $E_k$  is not sufficiently small, set

$$TOD_{k+1} = TOD_k - \frac{E_k(TOD_k - TOD_{k-1})}{E_k - E_{k-1}} \quad (4.2.5 - 1)$$

- f. and repeat steps (d) and (e)

In practice, this algorithm converges in 2 or 3 iterations. With complex weather patterns, it may take more, as these may introduce discontinuities in the relationship between TOD and total length of descent. The program also limits the number of iterations to some large number (such as 50) in order to guard against endless loops (if these limits are reached; the trajectory generation process is abandoned).

This yields the four-dimensional trajectory, which can be used in the proposed experiments listed below.

### 4.3 Use of Weather Forecast Models

A weather model (temperatures, pressures and wind speed) is essential for trajectory generating. The current state of the practice uses the current weather model for the entire trajectory generation



process, even though the trajectory itself may span many hours. NOAA provides not only the current hour weather model, but predictions for future hours as well.

This experiment modifies the trajectory generation process to use those forecast models, interpolating between hours to get an approximation of the variables at the cusp times in the trajectory.

This increases the complexity (slightly) and the storage needed (more than slightly) of the algorithm, and the question to be answered is whether this substantially changes the produced trajectory, especially the duration of the trajectory.

The set of flights to analyze is chosen to span the range of short to long flights, and to cover the continental US airspace. The coverage of these flights is shown in Figure 5 Flights Paths for the Use of Forecasted Weather analysis.

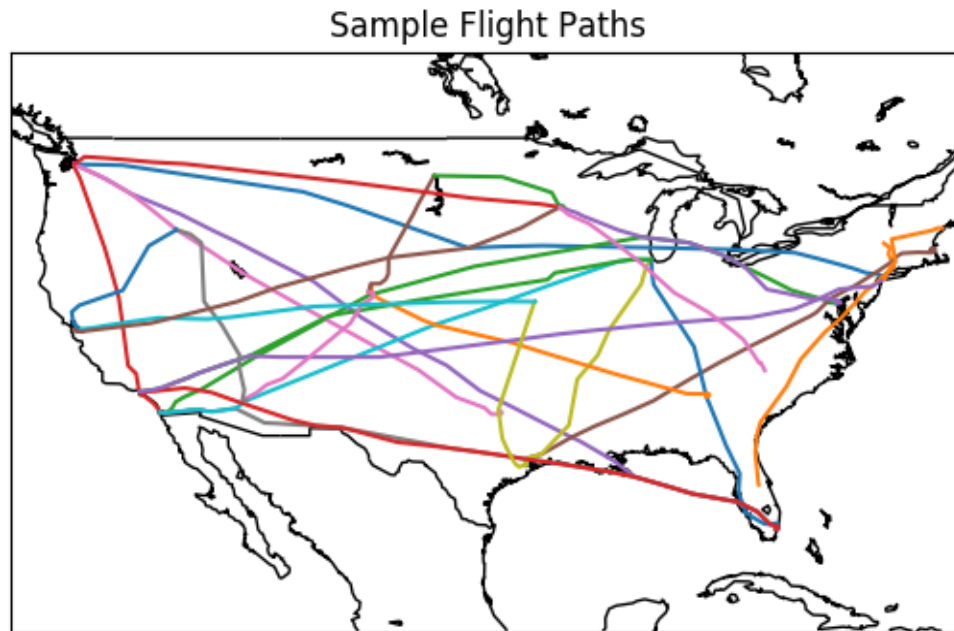


*Figure 5 Flights Paths for the Use of Forecasted Weather analysis*

#### 4.4 Wind Optimal Trajectories

The trajectories as described above follow a known path along the surface of the earth between waypoints. By following these paths, separating aircraft becomes somewhat simpler; especially to human air traffic controller who is used to aircraft following known paths.

By using the rigid path, however, the time in the air may be longer than necessary, especially if there are favorable wind conditions on other paths. This experiment will use Particle Swarm Optimization (PSO) techniques [4][5] to find an optimal path from fixed end points (the departure and destination airports are fixed, obviously). In this case, “optimal” can be defined as a function by an airline operator; the simplest choices are total flight time or fuel burned.

Note that there have been debates in the air traffic community about so-called “free flight” (letting aircraft fly where they want to, rather than where the air traffic control system dictates). This experiment will make no assumption on the future plans of the FAA to encourage or discourage free flight; rather the emphasis is applying PSO to this problem space.

PSO is used to find paths between two points (A and B in this discussion). Since the initial departure path from an airport is determined by available runways and wind conditions, point A will start at what is called the “Meter Fix”; a point after departing the airport. Similarly, point B will be the meter fix on approach to the destination airport.

PSO examines several paths from A to B. A fuel usage value is calculated for each path, and PSO iterates until it appears that the improvements in additional paths is minimal. PSO doesn't guarantee that a minimum value is found; rather the goal is to find an acceptable solution in a relatively small amount of time.

This work has been included in the paper “Wind Optimal Trajectories for UAS and Light Aircraft”, to be presented at the Digital Avionics Systems Conference in September 2017. Please refer to that paper for a complete description of the final algorithm. Contained below is a description of an initial implementation and the final implementation as detailed in the referenced paper.

#### 4.4.1 Version 1

The algorithm contains a bit of randomness (simulating the somewhat random behavior of a swarm), but learns from each iteration as to where the next iteration should concentrate. The basic operation of the PSO algorithm is shown in Figure 6.

One iteration of the algorithm will find many paths. Any given path is determined by a set of points. Figure 6 shows 5 possible paths starting at point A. The first iteration always proceeds this way; the number of paths and the range covered by those paths will be determined by experimentation. One segment in one path is a straight line of a given distance, ending at point P in the figure. The next segment will be of the same length; the direction of the segment is constructed based on three values:

- 1) The course coming into point P. This is called  $\Theta_i$  (for inertia). There is some randomness introduced into this value, within a range +/- around the incoming course.
- 2) The course with the optimal tail wind at point P. This is called  $\Theta_w$  (for wind). Recall that the wind values are in a three-dimensional grid, so altitude matters when determining the wind. For the departure segments from point A, altitude is determined from the ROCD calculations given in section 4.2.3. For approach segments to point B, this is more difficult as the general algorithm includes an iterative approach to find the top of descent point (section 4.2.5). As an approximation, a standard descent profile is built in the absence of winds, going from the cruise altitude to the altitude of point B, and once a new point P is within that (direct) distance of B, the altitude is retrieved from that standard profile at the distance (P -> B) from the end point.

3) The course from P to the endpoint B. This is called  $\Theta_e$  (for end point).

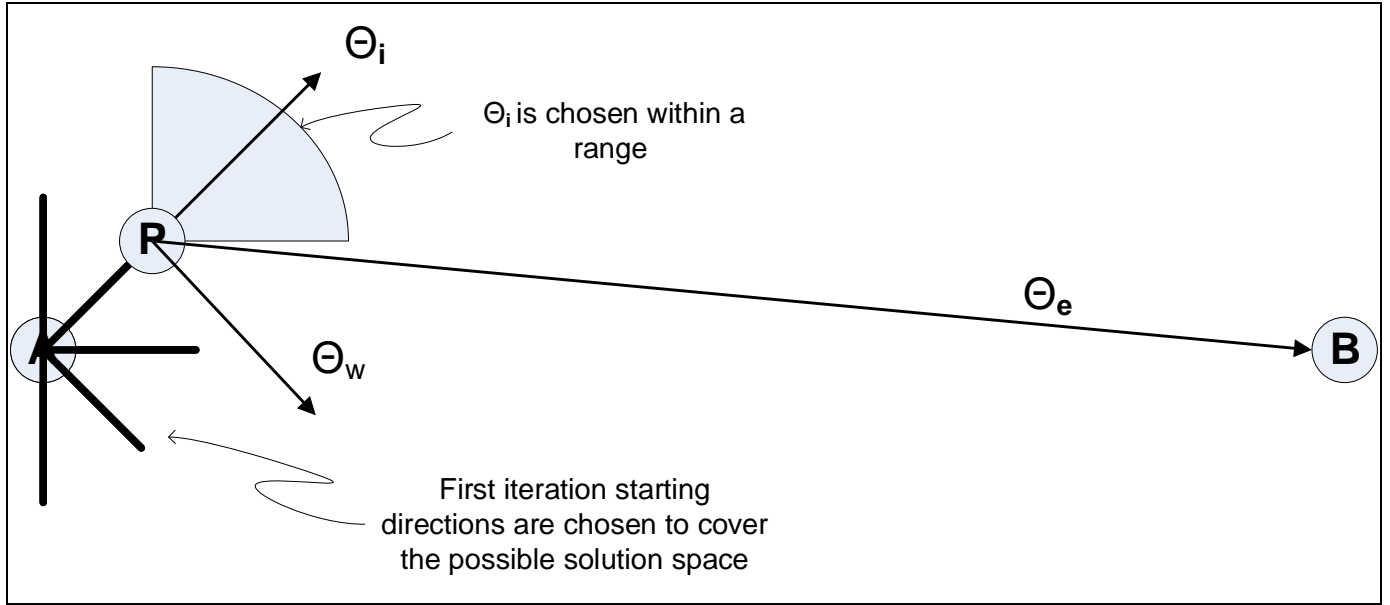


Figure 6 Wind Optimal Trajectories, Version 1

These three courses are combined with a set of weights:

$$\theta = W_i \theta_i + W_e \theta_e + W_w \theta_w \quad (4.4.1 - 1)$$

These weights sum to 1.0. In order to converge on B, the weights are calculated as follows.

$W_e$  is calculated first, according to how close we are to the endpoint:

$$W_e = \left( 1 - \frac{\text{dist}(P, B)}{\text{dist}(A, B)} \right) \quad (4.4.1 - 2)$$

Additionally, once  $W_e$  is greater than a threshold (say, 0.95), it will be set to 1.0. This ensures we eventually get directly to point B.

Once  $W_e$  is known, the remaining weight ( $1.0 - W_e$ ) is divided between  $W_i$  and  $W_w$  based on pre-determined percentages; say 70% for wind and 30% for inertia. This ratio is subject to experimentation.

When the ultimate course  $\theta$  is known, a new point P can be calculated as the next step on the path.

Each path in the iteration is calculated in this fashion. This will result in a set of zig-zag lines. These lines are smoothed to represent flyable paths, and the fuel consumption for each path is calculated.

That concludes one iteration. The lowest-fuel consumption path is chosen as the "best" path for that iteration.

Any iterations after the first differ only in the starting courses. Since a previous best path is known, the starting courses from point A are now chosen to cluster around that previous best path.

Iterations proceed until the delta fuel usage for the best path between iterations is less than some selectable value epsilon.

#### 4.4.2 Version 2

Several deficiencies were noted in version 1:

- Head wind situation – first approach zero-ed out wind weight when flying into head wind. This ignores some valuable information, as forward ground speed can still be optimized
- Magnitude of wind – first approach did not factor magnitude of the wind, just the direction
- Large perpendicular deviations – first approach did not penalize paths that were far off the direct A-B path
- Smooth Behavior – first approach had some step functions (such as zeroing wind for head winds) that gives discontinuous results. Sigmoid functions are used instead of step functions to give smooth results

These were addressed by changing the method used to find the course to the next point; the equivalent of the formula shown in 4.4.1-1.

In this formulation, a standard sigmoid function is used in a few places; the sigmoid function is defined as:

$$Sig(x) = \frac{1}{1 + \exp\left(\frac{midpoint - x}{slope}\right)} \quad (4.4.2 - 1)$$

The midpoint and slope values for each use of the sigmoid are tuned via experimentation.

The revised algorithm finds the next course as follows (refer to Figure 7 Wind Optimal Trajectories for the definition of terms).

$$\theta = W_i \theta_f + W_e \theta_e \quad (4.4.2 - 2)$$

where

$$W_e = q^2 + s * Sig(q) \quad (4.4.2 - 3)$$

$$q = \frac{d_{parallel}}{d_{AB}}$$

$$s = \frac{d_{perp}}{D}, \text{ where } D = \text{constant } 20 \text{ nautical miles}$$

$$\text{Normalize: } W_e = \frac{W_e}{1+s}$$

$$\theta_f = \theta_i + (+/- 30^\circ) * Sig(u) \quad (4.4.2 - 4)$$

$$u = \frac{\text{Wind Speed Along Path}}{V_{TAS}}$$

$$1 = W_i + W_e \quad (4.4.2 - 5)$$

(this allows  $W_i$  to be found once  $W_e$  is known)

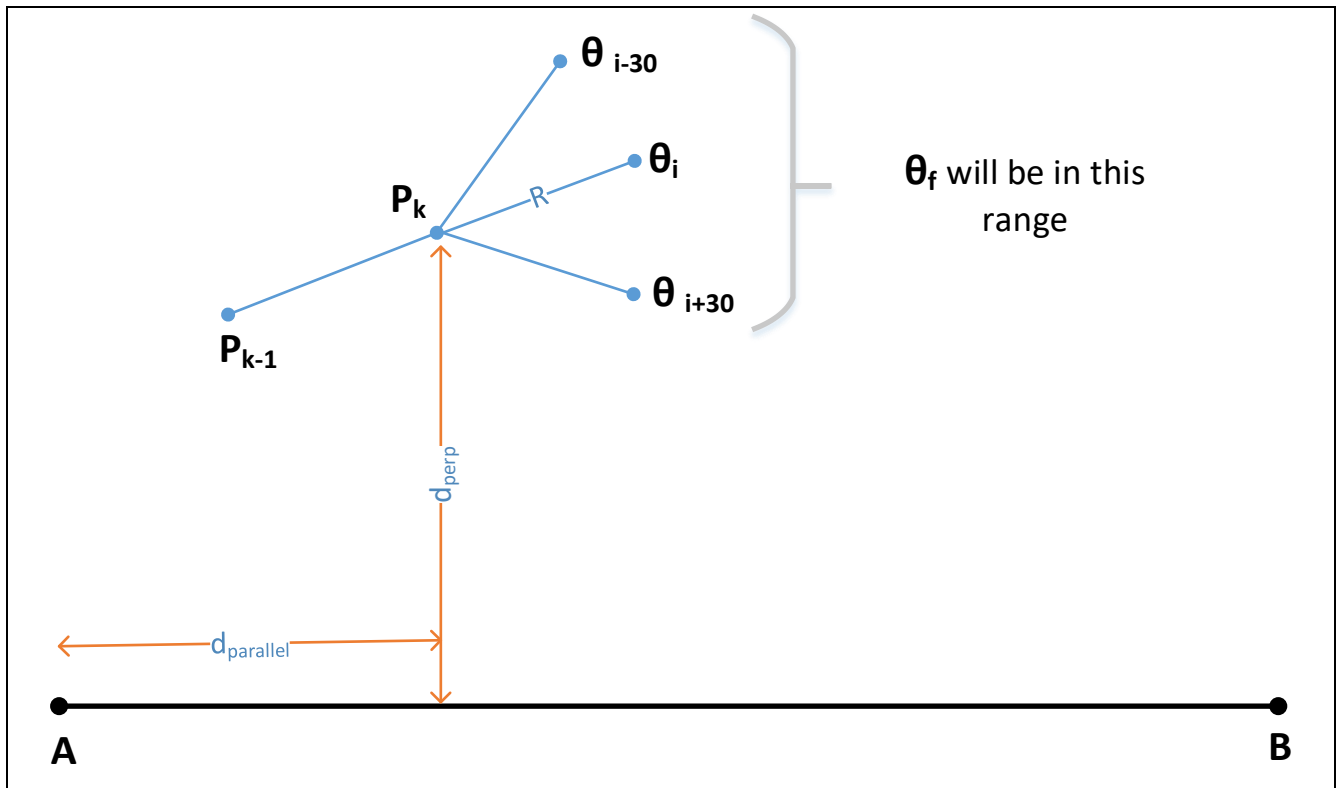


Figure 7 Wind Optimal Trajectories, Version 2

The other parts of the algorithm (iterations, multiple paths, etc) remained unchanged from version 1.

#### 4.5 Parallelizing Conflict Detection

Once a flight information region has a set of trajectories (flights that are currently airborne or are scheduled to be airborne within some time horizon), the ATC systems must predict if any two aircraft will come too close to one another, or if any aircraft will enter restricted airspace.

The aircraft-to-aircraft case is interesting in that it is a compute-intensive activity that might lend itself to parallelization. At its core, this process must compare any new or changed trajectory against all other trajectories in the FIR's set of flights. Since each trajectory consists of a set of segments, this entails many segment-to-segment comparisons. A typical FIR may have 200 or so flights in its working set, each of those trajectories may have 200 or so segments. A completely brute force approach would then, for a single new or modified flight, do 200 (segments in new trajectory) x 200 x 200 (segments in existing trajectories), or 8,000,000 comparisons.

In practice [7], this is implemented as a sequential process where the vast number of comparisons is reduced by a set of filters (the filters weed out cases that could not possibly be in conflict). The first two filters listed below are on the trajectories as a whole; the remaining are for each segment on the two trajectories being checked.

In the production system, these filters are:

- 1) Trajectory level coarse time filter – if one trajectory ends before the other starts, they cannot be in conflict
- 2) Trajectory level box filter – this compares the “box” constructed in three dimensions (latitude, longitude and altitude) for each of the two trajectories being compared, to see if there is overlap at that level
- 3) Segment level vertical coarse filter – this checks to see if the two segments are within the same altitude band
- 4) Segment level horizontal coarse filter – this checks the minimum approach distance in a horizontal direction
- 5) Segment level horizontal middle filter – again checks for closest approach, but now considers where the aircraft might be within the segment
- 6) Segment level vertical middle filter – again considers altitude, but only on the portion of the segments that come within the horizontal separation distances
- 7) Segment level horizontal fine filter – checks for closest approach, but only the regions that have passed the previous filters

A true conflict is one that passes all filters. As mentioned above, the first two are trajectory-wide and would not be affected by parallelization, so are not further considered. The complexity of the remaining filters is somewhat driven by the processing power available when this method was conceived (the early 1990s). The essential steps, which are described here, are:

- 1) A time filter; do the segments overlap in time?
- 2) An altitude filter; are the segments within the desired separation distance in altitude?
- 3) A horizontal filter; do two segments that have proven to be within time and altitude separation, violate the lateral separation distance?

These three steps are contained in the prototype, and are described in further detail now. Recall that each filter is comparing a segment from a “new” trajectory (called the subject trajectory) with a segment from an existing trajectory (called the “object” trajectory).

#### 4.5.1 Time Filter

The time filter will eliminate segments that don't overlap in time at all, and for the remaining pairs, trim each segment to the start and end time of the overlap. As an example:

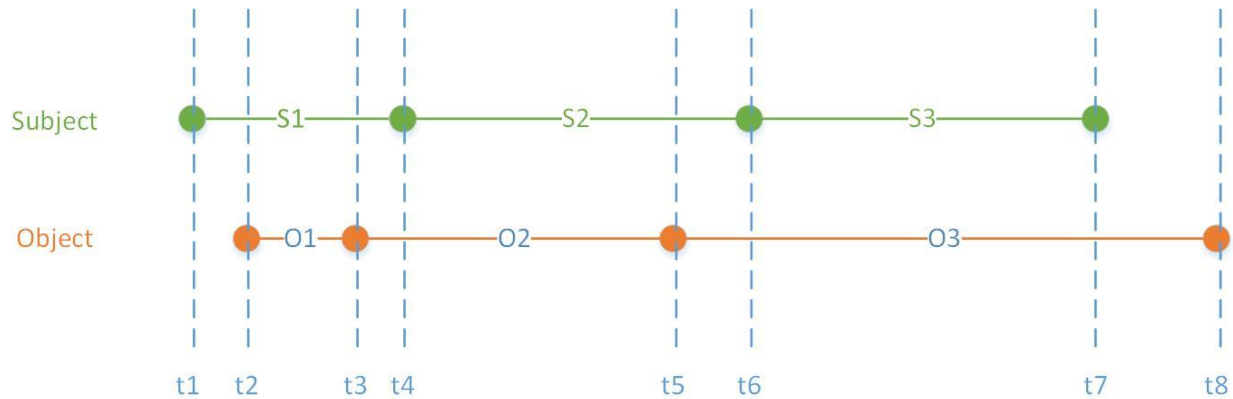


Figure 8 Conflict Detection Time Filter

After the time filter, the pairs that are still potentially in conflict are:

- 1) S1 and O1, from time t2 to t3
- 2) S1 and O2, from time t3 to t4
- 3) S2 and O2, from time t4 to t5
- 4) S2 and O3, from time t5 to t6
- 5) S3 and O3, from time t6 to t7

The trimmed segments that are still potentially in conflict are passed to the altitude filter.

##### 4.5.1.1 Altitude Filter

The altitude filter is now dealing with pairs of segments that start at the same time, and end at a later (same) time. The filter will retain any pairs that are within the separation altitude, and potentially again trim the segments so that they cover only the time when the separation standard would be violated.

As an example of this:

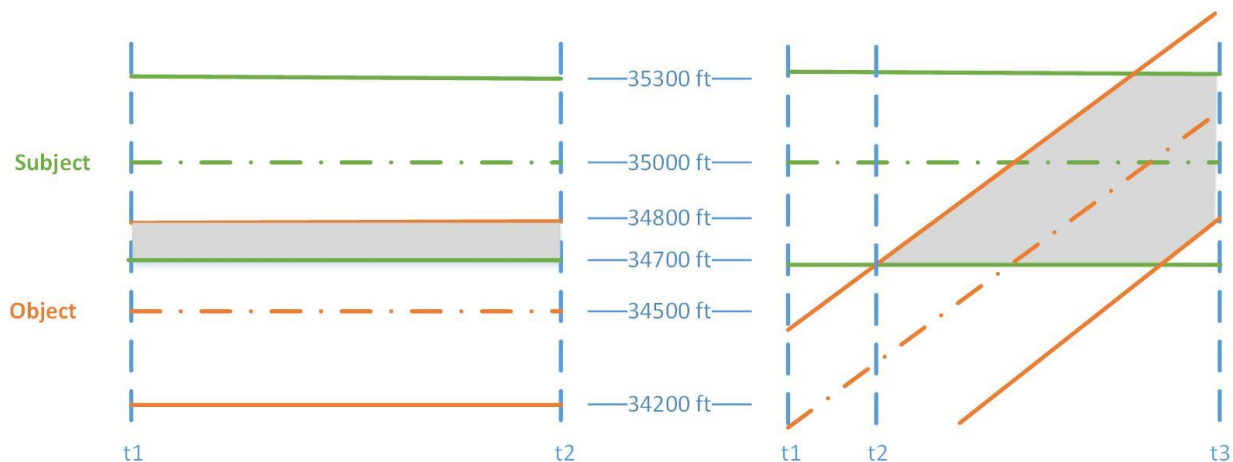


Figure 9 Conflict Detection Altitude Filter

In this example, the separation standard is 600 feet of altitude. A “band” around each segment is constructed at +/- half of the separation standard (in this case, +/- 300 feet). If the bands overlap (as shown by the shaded region in the figure), there is a potential conflict.

In the left-hand example, both flights are flying level, one at 35,000 feet and one at 34,500 feet. Since they are only 500 feet apart, they are potentially in conflict for the entire segment and no trimming is needed.

In the right-hand example, the object segment is climbing. The bands do not overlap for the entire interval, so each segment will be trimmed to start at  $t_2$  and at the existing end point ( $t_3$ ).

Any segments still potentially in conflict are passed to the horizontal filter after trimming.

#### 4.5.2 Horizontal Filter

The horizontal filter is the most complicated one, because it:

- 1) Compares two moving aircraft in the horizontal plane, and
- 2) Takes into account uncertainty in the aircraft’s position (this uncertainty is due to the fact that we are predicting aircraft movement into the future, and various elements, for example the wind, are not known with certainty). There is uncertainty in both forward/backward position and side-to-side position.

The method for doing this comparison follows several steps. We are starting with a pair of segments, each with two end points moving in some direction as shows in the left-hand side of this figure:

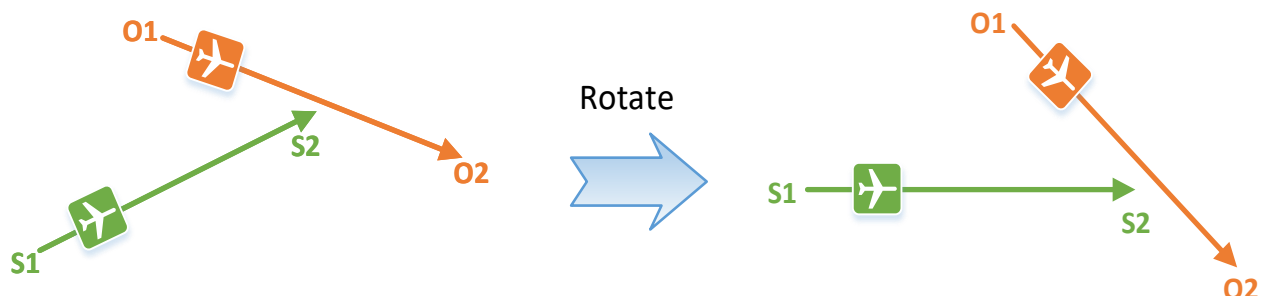


Figure 10 Conflict Detection Horizontal Filter - part 1

Up to now all positions have been expressed as a cartesian coordinate on sphere  $(x,y,z)$ . For short distances (which we have here), a stereographic projection of these positions is used making this a two-dimensional problem. The end point coordinates are projected onto a stereographic plane with tangent point of “S1”. Then all coordinates are rotated so that the subject segment lies on the X axis, with point S1 at location  $(0,0)$ .

Next, the problem is shifted to the subject aircraft’s point of view, and the object segment is drawn relative to a stationary subject aircraft at point S1:



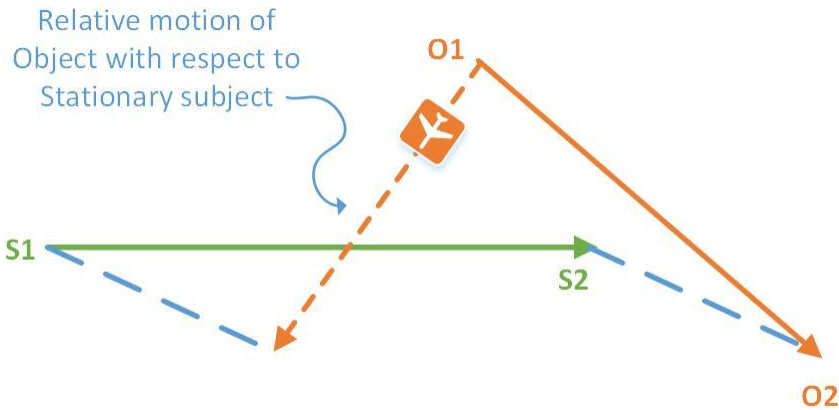


Figure 11 Conflict Detection Horizontal Filter - part 2

At this point, a simplistic approach would draw a circle with a radius of the horizontal standard (5 Nmi) around the subject point, and see if the object segment intersected that circle. However, this doesn't account of the positional uncertainty. To do that, first a rectangle depicting the forward-backward and side-to-side uncertainty is drawn around the subject position. At each of the corners of the rectangle, similar rectangles (in the direction of the original object aircraft) are drawn, as shown below. The outer edges of these rectangles show a region that, if avoided, account for the uncertainty in positions.



Figure 12 Conflict Detection Horizontal Filter - part 3

The outer edges form an octagon, as shown by the dotted line below:

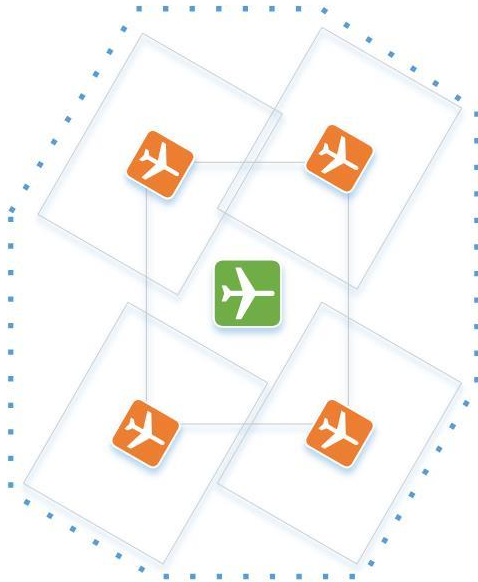


Figure 13 Conflict Detection Horizontal Filter - part 4

This region is expanded by the separation standard of 5 NMI:

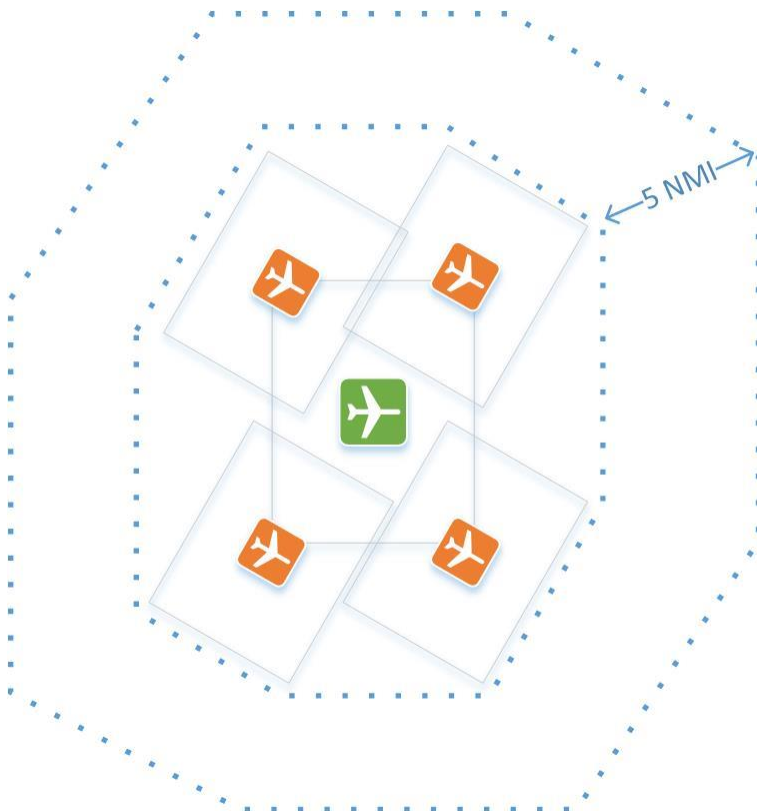


Figure 14 Conflict Detection Horizontal Filter - part 5

Finally, to evaluate the possible conflict, we see if the relative object segment (with respect to the stationary subject segment) intersections this outer octagon:

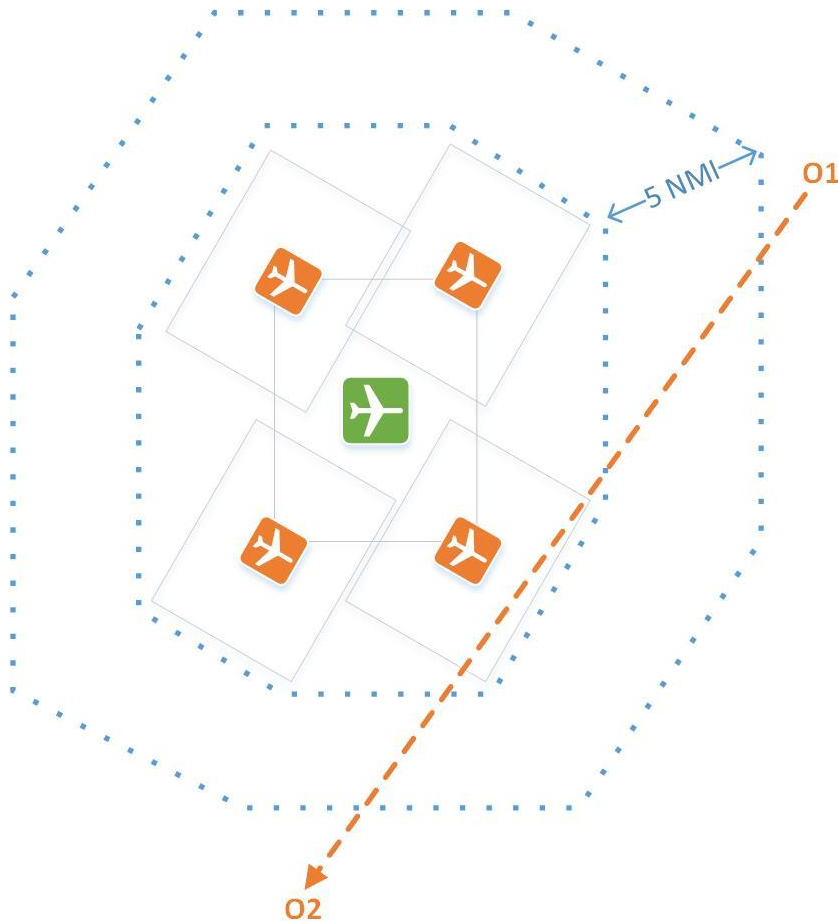


Figure 15 Conflict Detection Horizontal Filter - part 6

In this example, we would have a conflict, starting at where O1-O2 first intersects the octagon and ending where it exits the octagon at the bottom of the figure.

#### 4.5.3 Parallelization Strategies

Given this basic algorithm, the challenge in using the GPU is what kind of memory transfers are done between CPU and GPU (and back), and how much work is done by each “subroutine” (or kernel, in NVIDIA’s documentation). Figure 16 NVIDIA CPU/GPU Architecture shows the basic architecture of NVIDIA’s GPU display boards existing in a desktop PC. The conflict detection kernel that compares one segment to another segment is part of program structures that will eventually do  $A*B*C$  compares, where “A” is the total number of flights in the airspace, “B” is the average number of segments in the newly-introduced flight (the subject flight) and “C” is the average number of segments in the existing (object) flights. B and C are equal, so if we confine ourselves to one flight-to-flight compare, the problem includes  $B*C$  comparisons.

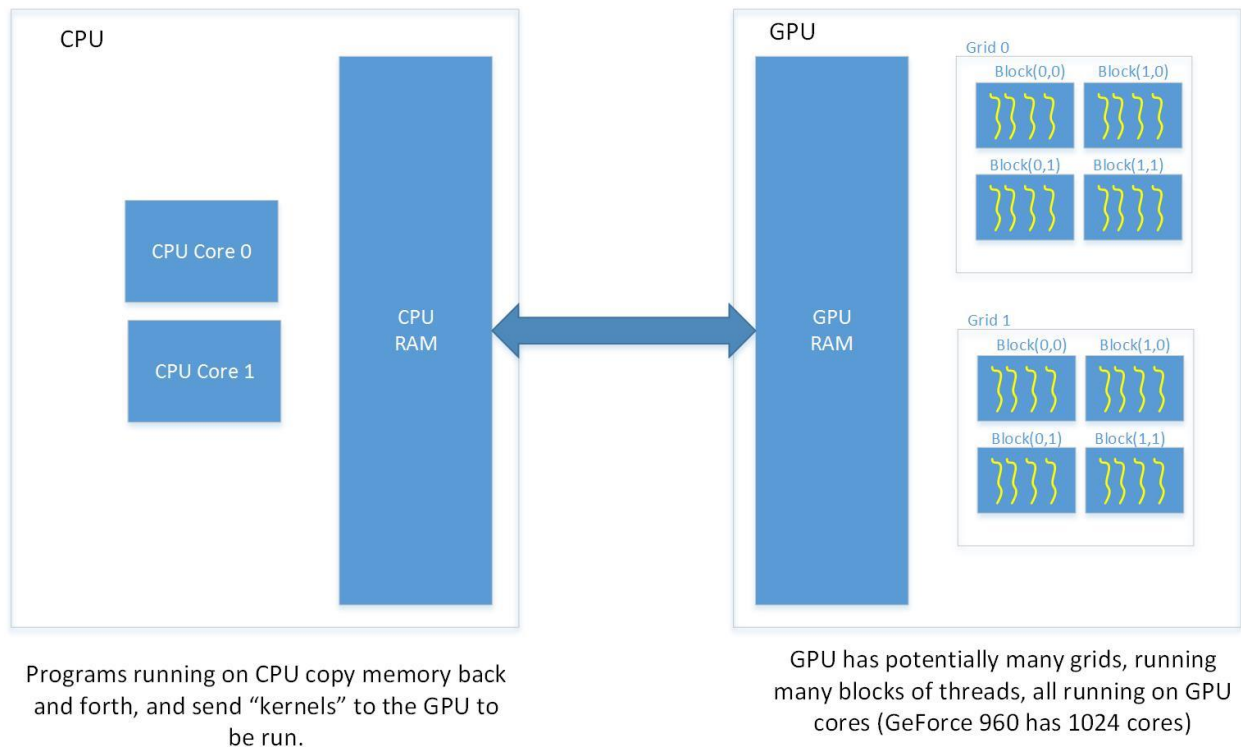


Figure 16 NVIDIA CPU/GPU Architecture

Three strategies were evaluated:

- 1) Have one call to a kernel done for each subject segment. This will mean that for any flight-to-flight comparison, “B” kernel calls will be made; each of those calls will do “C” compares. The results have to be communicated back to the CPU via a memory transfer across the CPU bus. With this design, there would be one block containing “C” threads (or alternatively “C” blocks with one thread each).
- 2) Have one call to a kernel done for each flight-to-flight comparison. Each kernel call does B\*C compares.  
With this design, there would be “B” blocks, each doing “C” compares. The results are copied back to the CPU at the conclusion, using this scheme show in Figure 17 Memory moves for strategy 2. Using this strategy, there is one memory move to get an array of counts of conflicts by subject segment (many of which will be zero). The a second set of memory moves, one for each subject segment that had conflicts. Finally, on the CPU, these conflicts are “consolidated” (that is, adjacent conflicts are merged into contiguous conflicts).
- 3) The same single kernel call is done as in option 2, but the design of the return values is slightly different. In this case, the consolidation is done on the GPU via a new kernel call (this kernel is run in just one grid/thread). A return parameter (which must be copied to the CPU) indicated how many consolidated conflicts there are, and a final memory move gets an array of that many conflicts.

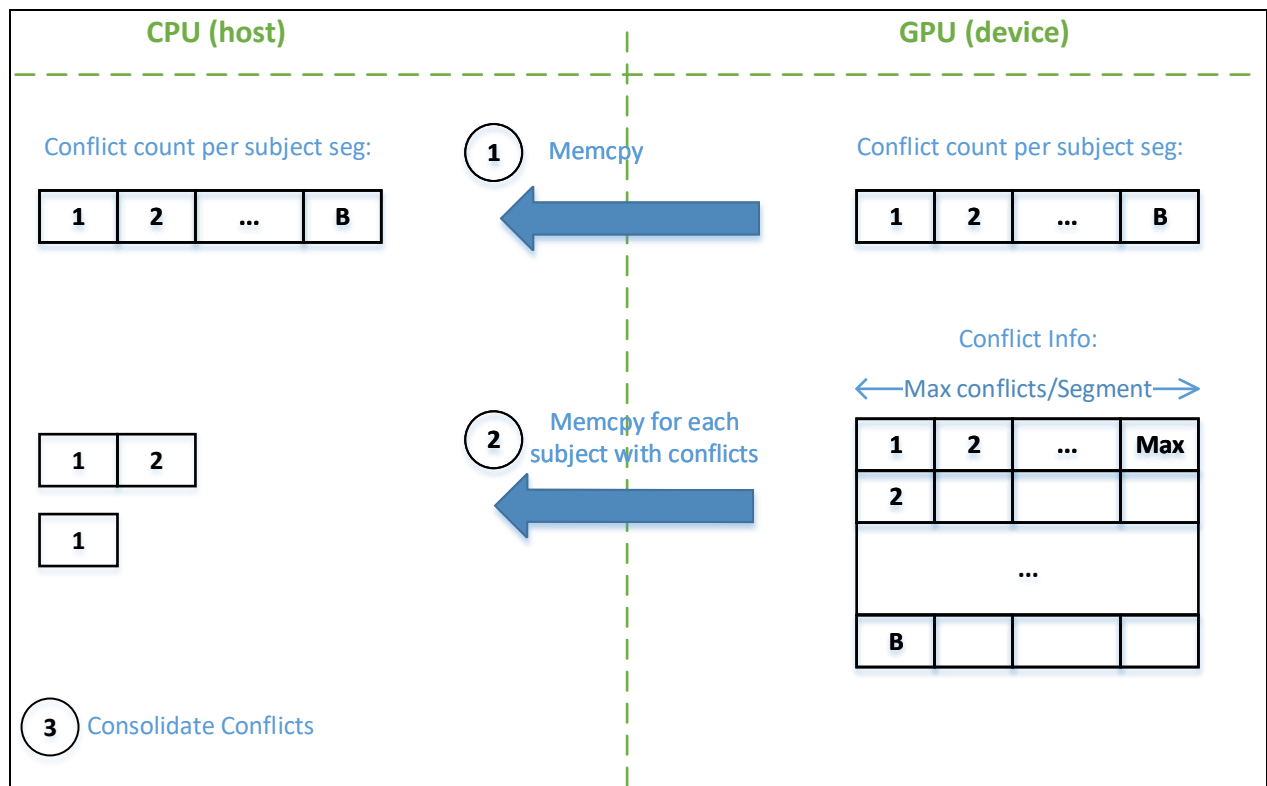


Figure 17 Memory moves for strategy 2

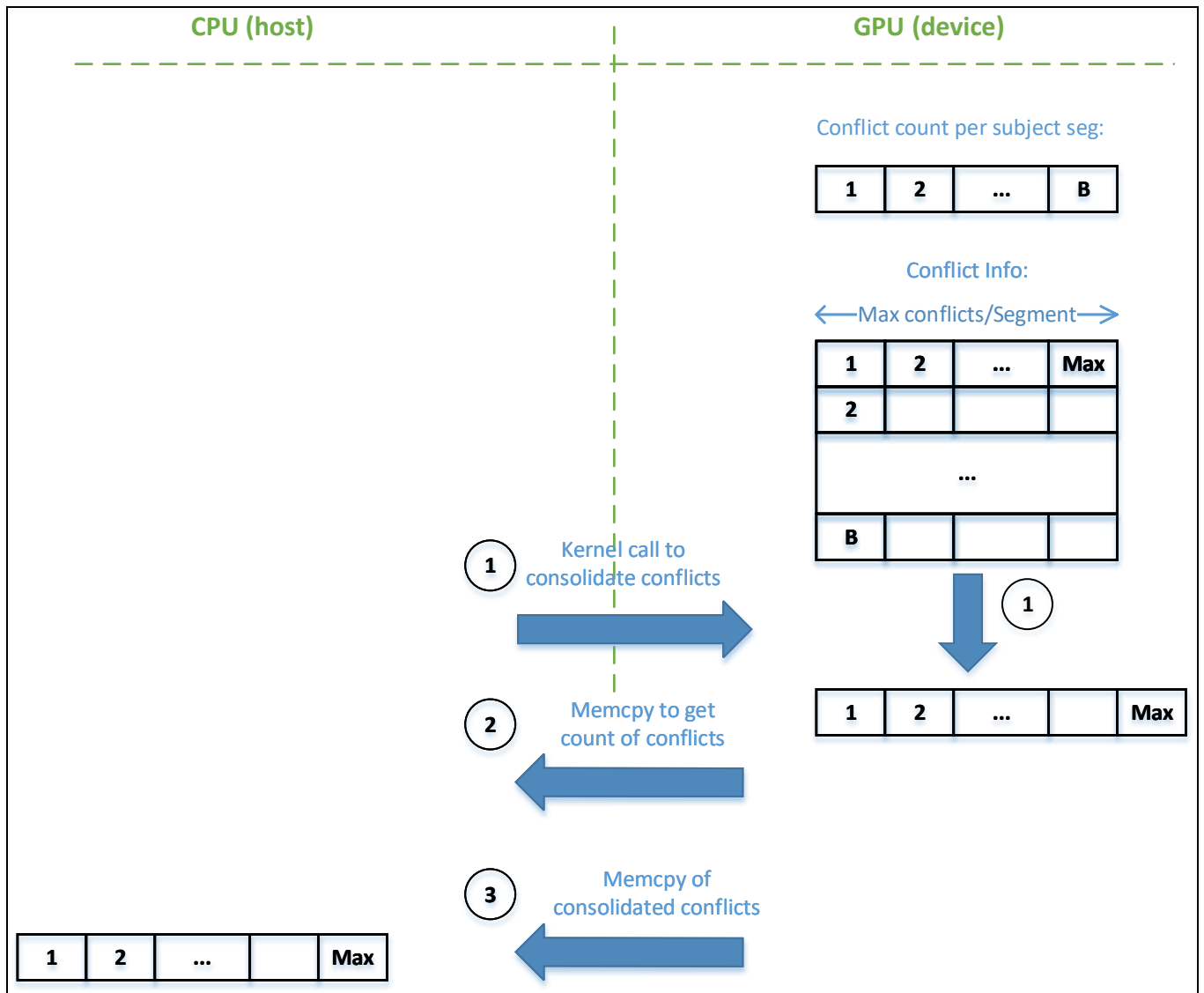


Figure 18 Memory moves for strategy 3

## 5 Implementation

Trajectory generation, Use of Forecasted Data and Wind Optimal Trajectories are implemented using the Python language. It offers the following advantages:

- Portable to many operating systems.
- Has the concepts of exception handling, classes, objects, modules, and packages.
- Has a wealth of other packages for scientific computing.

In spite of not being strongly typed or compiled before execution, this makes Python attractive for this effort.

For an IDE, the PyDev Eclipse plug-in [11] is used. Git [12] is used for configuration management. Python offers some limited documentation support in the language, but a separate design document is among the deliverables; this will discuss major code structure and design decisions.

The development platform is a personal computer (desktop). Tests will also be run on this configuration.

The parallel processing experiment utilizes the processing features of a Graphics Processing Unit (GPU). A sequential implementation is compared to the parallel implementation. For this experiment, the C language is chosen. In order to fairly compare running the algorithm sequentially vs. in a parallel configuration, the same language has to be used in both cases. Since the GPU must be programmed in C (even if a different language is used to express the algorithm, it will ultimately get converted to C code to run on the GPU), C is chosen for the CPU as well.

This is run on a desktop PC running windows, with an Nvidia GEFORCE 960 graphics card. The CPU has multiple cores, but only core is used for the sequential version. The desktop processor has Intel i7-6700 processors with 4 cores and a clock speed of 3.40 GHz. The GEFORCE 960 has 8 floating point processors with a clock speeds of 1.1 GHz.

## 6 Validation Methods

The experiments that use a trajectory will be validated through careful construction of test cases (using alternative computations to ensure the necessary conditions are created), and then running those test cases to be sure the desired result is obtained.

The basis for all this work is a valid trajectory. Trajectory verification occurs on two levels, and takes advantage of the fact that a known, proven implementation exists (from real air traffic control (ATC) systems). First, the low level equations for thrust, drag, etc., are verified against existing implementations of those equations (same inputs should produce the same outputs). Second, the overall trajectory that was generated is compared against a similar result from an ATC system simulator.

This overall comparison for a descent segment is shown in Figure 19.

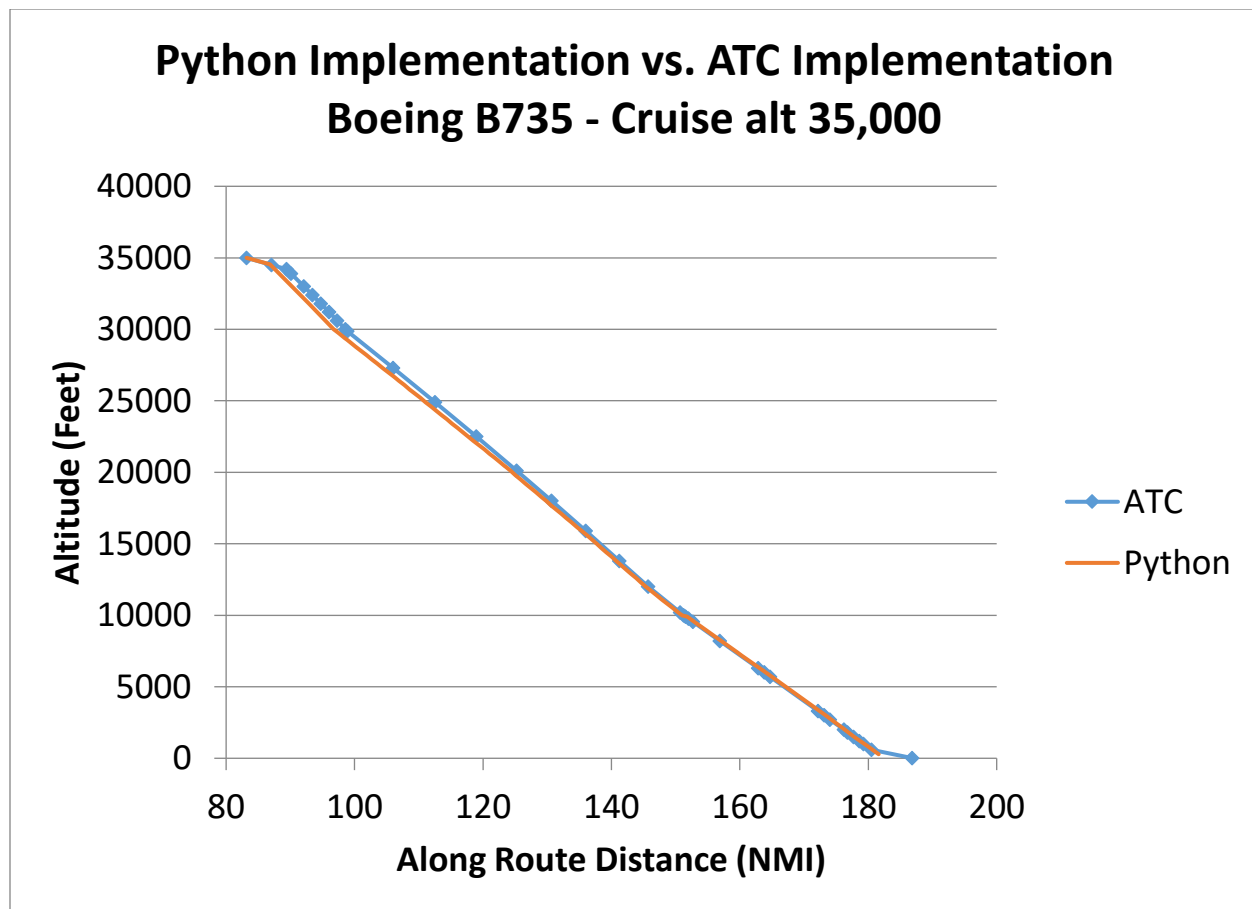


Figure 19 Trajectory Generation Comparison

There are two places where there are noticeable differences:

- 1) At the top of descent, both cases shown a period of acceleration, during which the desired descent speed is attained (this speed is different than the cruise speed of the aircraft, requiring this period of acceleration). During this period, the rate of descent will be smaller than normal, because energy is being used to change the speed. The Python generated trajectory ends this period sooner than the ATC version. A detailed analysis was undertaken for this; it revealed a bug in the ATC code (wrong value for acceleration was being used).
- 2) The Python generated trajectory ends sooner than the ATC trajectory. This is simply a function of the flight intent; the flight chosen for generation in Python was destined for an airport at 285 feet above sea level; the ATC flight was going to an airport at 14 feet above sea level. Hence the Python trajectory ends sooner.

The above comparison is done without any wind (in order to have a valid comparison, wind data must be equal, and there is no way to use the same wind conditions in both cases). Another test is needed to show that the wind speeds are applied properly. For this, a "windy" day was chosen, where there was a significant head wind in the Python flight's direction. This is expected to slow down the aircraft.



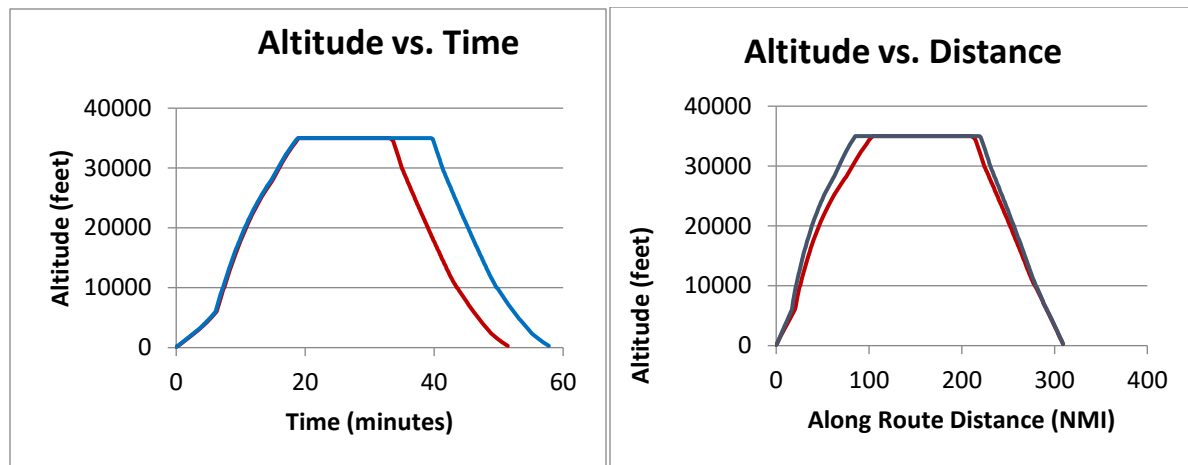


Figure 20 Effect of Wind on Trajectories

In both plots, the blue line is the trajectory with the head wind applied; the red line shows the same flight without wind. In an altitude vs. time plot, the climb and descent portions are identical (since the calculation of rate of climb/descent (Equation 4-5.4) does not depend on ground speed, only true airspeed). However, in this case, the cruise segment is elongated by more than 6 minutes due to the head wind. The same information presented as an altitude vs. distance plot shows the flight is at cruise for a longer distance, as the ground speed at cruise is reduced by the head wind.

## 7 Test Problems for Verification

### 7.1 Use of Weather Forecast Models

Several months of real weather models has been obtained from NOAA. Starting with the same flight intent input, several trajectories are generated using both the current forecast only and the future forecasts. These trajectories are chosen to traverse the FIR in different directions, in order to experience head and tail winds (see Figure 5 Flights Paths for the Use of Forecasted Weather analysis).

The total flight time of each flight will be compared.

### 7.2 Wind Optimal Trajectories

Using both the weather models used above and synthetic models designed to have greatly varying wind speeds in different regions, the Particle Swarm Optimization techniques will be used on a single flight.

### 7.3 Parallelizing Conflict Detection

An entire set of flights, as typically would be found in a FIR, is not needed for this experiment. Rather, we just need pairs of flights that show various degrees of “closeness” to being in conflict with one another. These are run through both a sequential algorithm and the parallel algorithm. Conflicts detected should be identical, and processing times can be compared. Since we are measuring both CPU and GPU time, the same experiment was run many times and wall clock time from beginning to end was compared.

A small set of conflicting flights was created, one pair of which has a lengthy conflict, as shown in Figure 21 Test flights used for Conflict Detection (the red flight and the orange flight conflict for a long period of time in that diagram). The other pairs have typical fairly short overlaps.

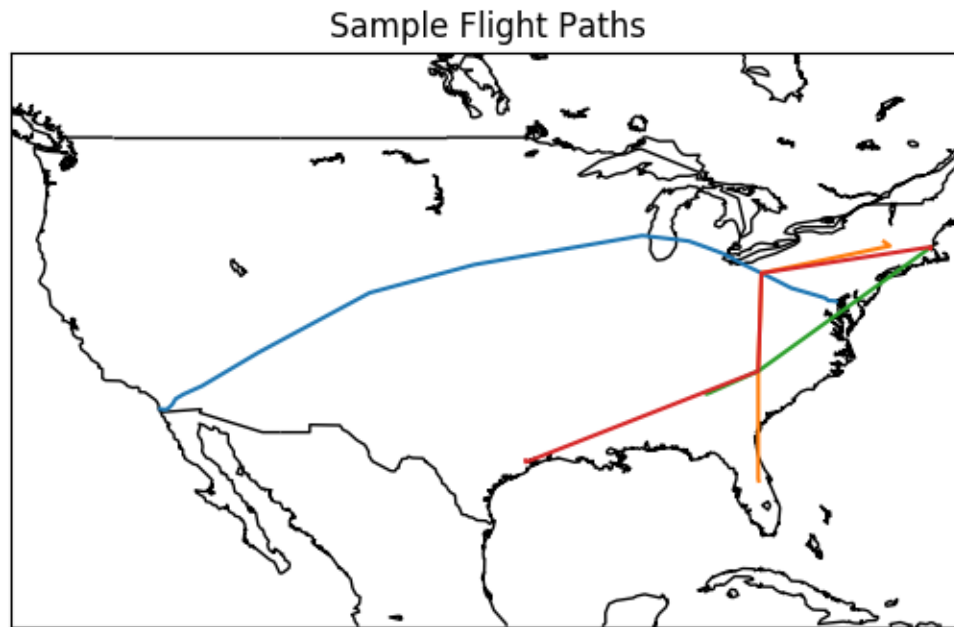


*Figure 21 Test flights used for Conflict Detection*

## 8 Results

### 8.1 Use of Weather Forecasts

Several flights of varying lengths and directions across the continental US were processed versus several months of weather data (usually 4 samples of weather collected per day). Not all days or all hours in a day were collected due to occasional connectivity issues to the NOAA web site.

#### 8.1.1 Quality of Forecast

The first question to be asked when proposing the use of a forecasted model is how good that forecast is. To evaluate this question, the difference between wind speed forecasted at time T for time T+5 hours and the actual wind reported at time T+5 hours calculated. Data was collected over several days and several hours in a day. The results vary by geography over the country. Figure 22 Accuracy of Forecasted Wind Speed shows a plot of the difference in magnitude of wind speed (regardless of direction of the wind).

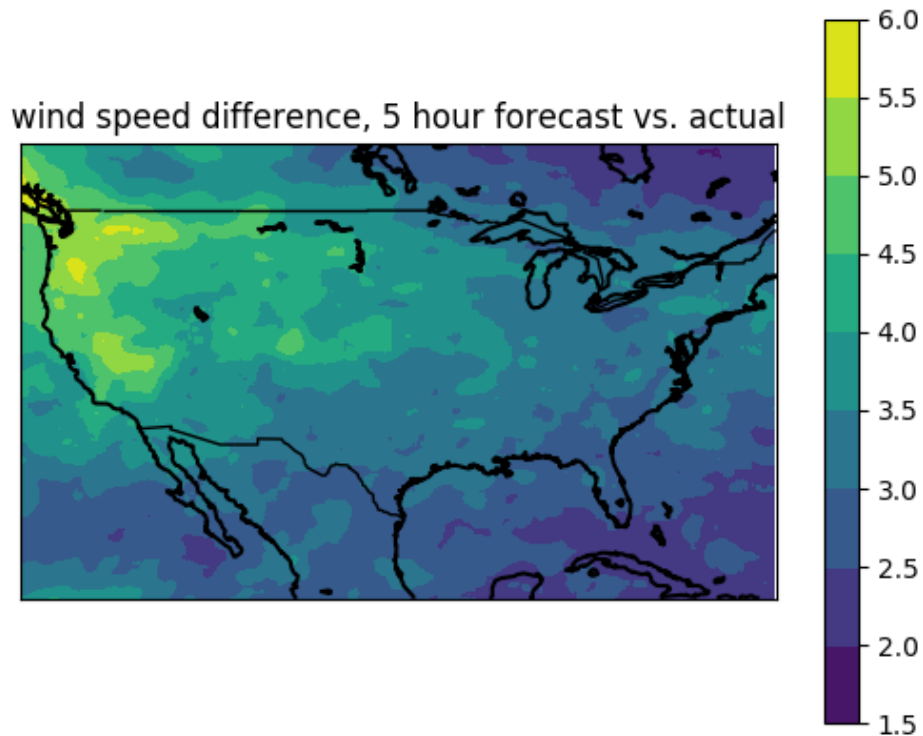


*Figure 22 Accuracy of Forecasted Wind Speed*

The upper northwest has the least accurate forecasts, probably due to the relatively fewer number of sensors in that area.

A flight traveling across country, with a continuous error of 3 knots in typical cruise speed of 420 knots would be 2 minutes off in total flight time. In practice, however, these errors aren't continuous, and in some cases cancel each other out (some forecasts are too fast, some are too slow). In addition, flights rarely fly directly into a headwind or ahead of a tail wind. Analysis of the data shows that the forecast error accounts for at most 0.2 minutes of flight time, which is acceptable when we are looking for differences of two to three minutes.

#### 8.1.2 Impact on Flight Time

Each flight in our set was analyzed against more than 400 weather samples. For each flight, results such as shown in Figure 23 Distribution of flight time differences with forecasted weather is obtained, which shows, for this one flight, the percentage of flights that are different by a particular amount. Two points are highlighted; a difference of 2 minutes and a difference of 3 minutes. The scheduling of flights is done in "slots" of one minute in duration. For the busiest airports, these slots are scheduled to be full, so an error big enough to move to a different slot will cause scheduling problems (the schedule will have to be adjusted in real time by having flights speed up, slow down or go into hold patterns). A flight that

is off by 2 minutes will need to go to a different slot, and one off by 3 minutes will certainly cause more re-ordering issues.

For the particular flight shown in the figure, about 25% of the instances of this flight will be off by two minutes or more, and about 13% will be off by 3 minutes or more.

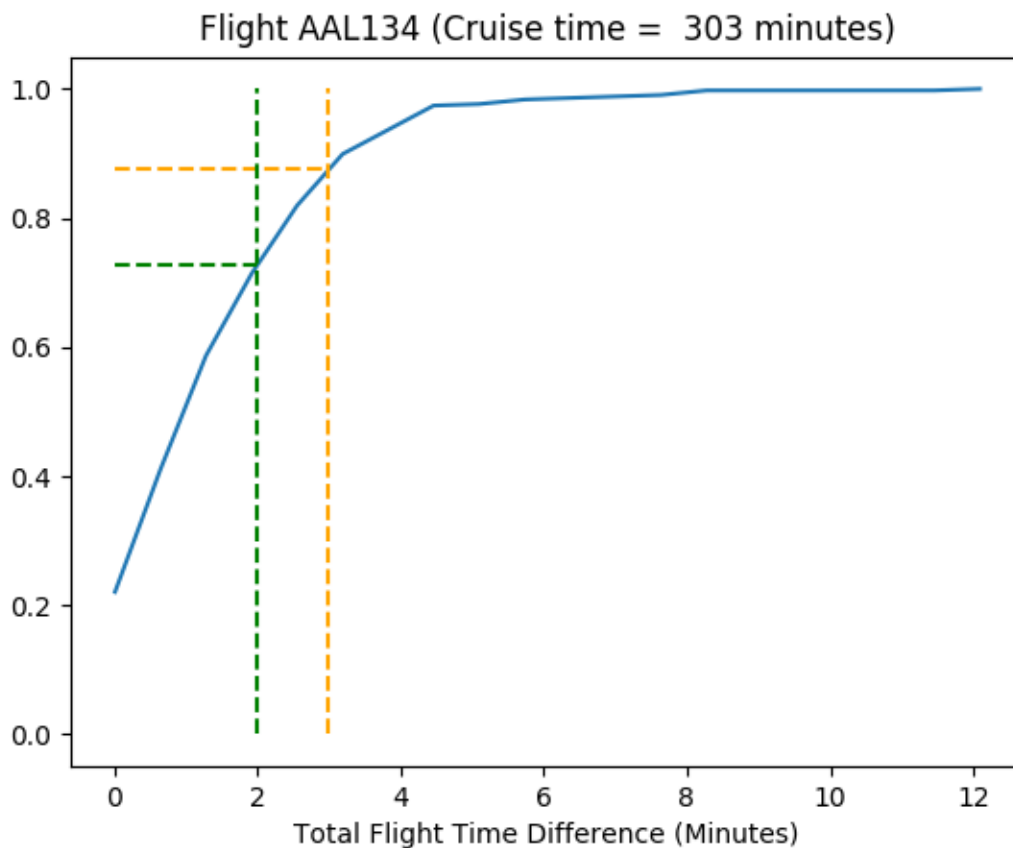


Figure 23 Distribution of flight time differences with forecasted weather

As one might expect, the error in flight time is greater for longer flights. For all the flights examined, an aggregate picture of percent of flights exceeding the two and three minute thresholds can be found in Figure 24 Summary of Flight Time Errors. This figure shows both the individual points and a trend line created by fitting a second-order polynomial to the data. From this we can see that for longer flights (4 hours or more), we can expect 8% to be off by at least 3 minutes. This is a significant number, and would argue that the increased precision that comes from using the forecasted data is merited in applications that use predictions for these medium or long duration flights.

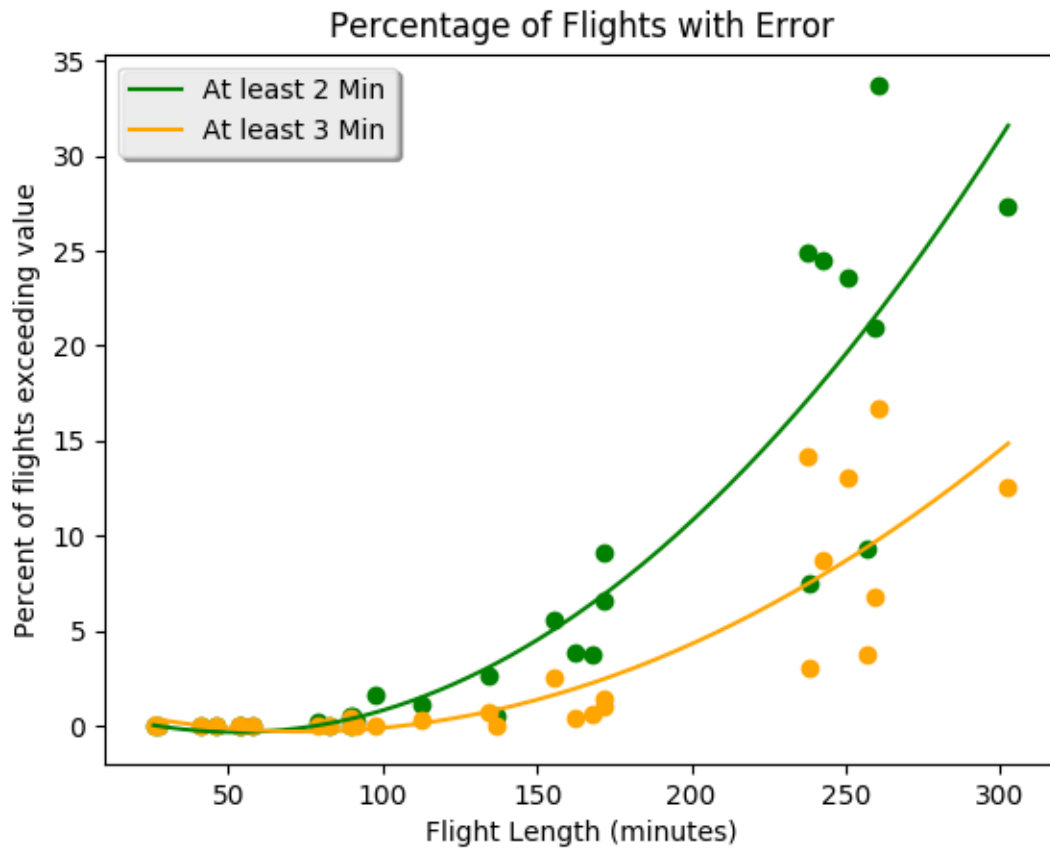


Figure 24 Summary of Flight Time Errors

## 8.2 Wind Optimal Trajectories

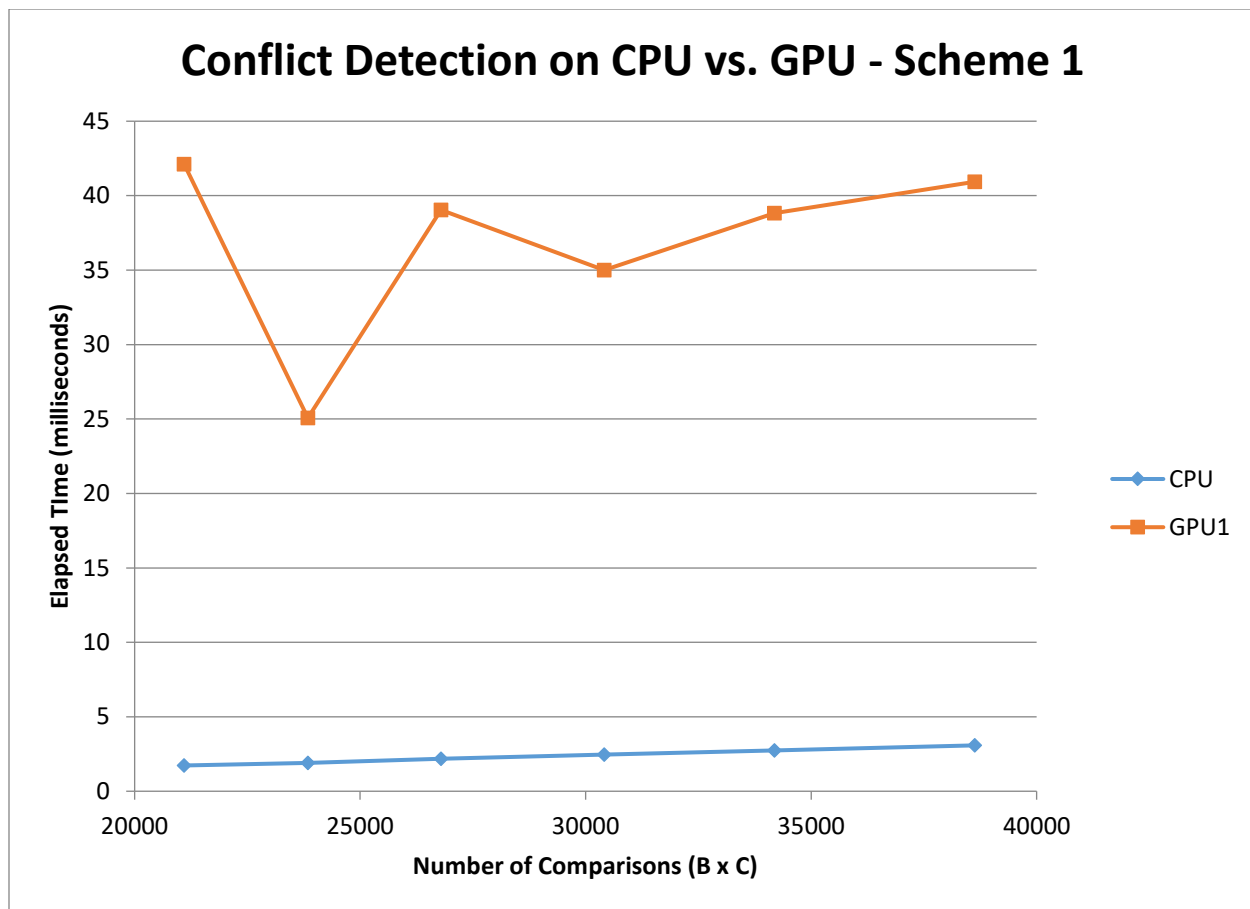
Optimal wind-aided trajectories should find “less expensive” trajectories than the nominal case. The reduction in expense can be quantified. In addition, examining some real NOAA data can show how likely it is that alternate, less expensive routes can be found.

## 8.3 Parallel Processing

As each scheme was coded, it was measured and compared against the same processing being done strictly in the CPU. The flight and conflict characteristics of the flights in conflict are summarized here:

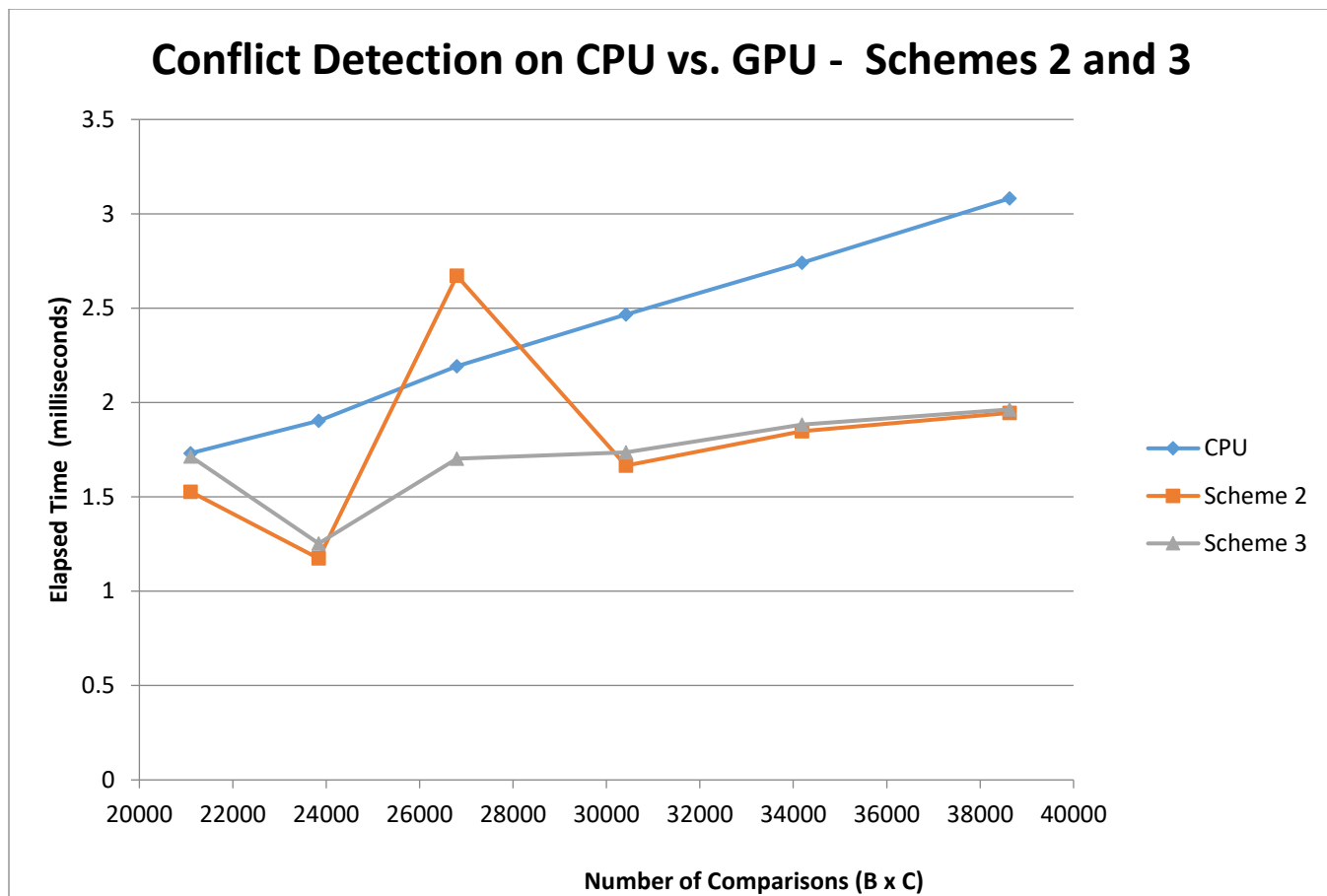
Subject Segs (B)	Object Segs (C)	B x C	Subject Segs in Conflict	Seg Pairs in Conflict
137	154	21098	1	2
174	137	23838	4	8
174	154	26796	27	52
137	222	30414	0	0
222	154	34188	2	4
174	222	38628	2	4

Scheme 1, which made one kernel call for each subject segment, is compared against a CPU-only solution:



In this scheme, the kernel invocation overhead dominates and the GPU version performs much worse than the CPU only version.

Schemes 2 and 3 reduce that kernel overhead by making just one call to do all comparisons:



The CPU line shows a fairly linear relationship between the number of comparisons and run time. Schemes 2 and 3 have generally reduced the time to below what is achievable on the CPU, except for the case with 26,796 comparisons. This is the case where there are many segments in conflicts. Scheme 2 will therefore do many array copies from GPU to CPU, and that copy overhead spikes the execution time.

Scheme 3 moderates that overhead at the expense of a small amount of processing on the GPU for conflict consolidation.

The GPU execution time also is growing with a flatter slope than the CPU scheme, probably because it can better interleave short kernel executions with longer ones, while we are only using one core, and hence one instruction pipeline, on the CPU.

Future work could serve to lower the GPU numbers more, by perhaps running all  $A*B*C$  comparisons with one kernel call (utilizing several more grids) or perhaps using faster memory in the GPU (the GPU has several difference classes of memory, all but the most general is limited in size or scope, and the fastest is limited to being read-only in the GPU).

## 9 Conclusion

The creation of a framework to produce trajectories, given the parameters found in a BADA dataset, can be used for many experiments of interest to ATC. This project established that framework and conducted a few such experiments. These experiments were designed to provide insight into situations confronting ATC today, and the framework can continue to be used for future work.

The primary benefit was to establish the framework and show experiments can effectively use it.

The “Use of Forecasted Weather” experiment has shown that for flights of longer than 3 hours, forecasted weather will improve the estimates of arrival at the destination meter fix by enough that it should be used; Figure 24 Summary of Flight Time Errors shows that 10% of flights of 3 hours or more will be off by at least 2 minutes.

The “Wind Optimal Trajectories” experiment shows that, for light aircraft such as unmanned aerial vehicles (drones), where the aircraft’s speed is not much greater than the fastest wind speed encountered, a wind optimal trajectory can save significant time. The method presented is a compute-efficient way to find those trajectories.

Finally, the “Parallel Conflict Probe” experiment shows that performance gains can be had by running parts of the conflict probe algorithm on the multiple cores in a GPU, and the CUDA framework provides a straight-forward way to do that.

## Appendix A. Timeline

*Table 1 Proposed Schedule*

Timeframe	Progress Achieved
Thanksgiving	Implement trajectory generation using BADA version 3 - <b>completed</b> Detail the particle swarm optimization algorithm to be used - <b>completed</b>
December	Implement and measure the use of forecasted weather- <b>completed</b>
January	Initial PSO algorithm for wind-aided trajectories- <b>completed</b>
February	Initial parallel conflict detection algorithm- <b>completed</b>
March	Additional parallel algorithm tests, tuning PSO algorithm- <b>completed</b>
May	Final algorithms and analysis, produce final report- <b>completed</b>
If time allows	Implement BADA 4, compare BADA 3 vs 4 – <b>not attempted</b>

## Appendix B. Milestones

The milestones roughly follow the schedule presented, including these items:

- 1) Basic Trajectory Generation algorithm implemented and tested
- 2) Initial version of each algorithm implemented
- 3) Final version of each algorithm implemented and tested



- 4) Final report produced

## Appendix C. Deliverables

- 1) Python/C Source Code, with comments
- 2) Design documentation to augment commented code
- 3) Results
- 4) Class presentations and reports
- 5) Draft papers, to be presented at the DASC conference in September 2017

## Appendix D. Bibliography

1.	Eurocontrol Base of Aircraft Data (BADA), <a href="http://www.eurocontrol.int/services/bada">http://www.eurocontrol.int/services/bada</a>
2.	"World Geodetic System – 1984", <a href="http://www.unoosa.org/pdf/icg/2012/template/WGS_84.pdf">www.unoosa.org/pdf/icg/2012/template/WGS_84.pdf</a>
3.	Aircraft Modelling Standards for Future ATC Systems; EUROCONTROL Division E1, Document No. 872003
4.	Kennedy, J. and Eberhart, R. C. Particle swarm optimization. Proc. IEEE int'l conf. on neural networks Vol. IV, pp. 1942-1948. IEEE service center, Piscataway, NJ, 1995.
5.	<a href="http://www.swarmintelligence.org/tutorials.php">http://www.swarmintelligence.org/tutorials.php</a>
6.	GRid in Binary (GRIB), the World Meteorological Organization (WMO) Standard for Gridded Data, <a href="http://dao.gsfc.nasa.gov/data_stuff/formatPages/GRIB.html">http://dao.gsfc.nasa.gov/data_stuff/formatPages/GRIB.html</a>
7.	"ERAM Conflict Management, Off-Line Problem Determination, and Utility Algorithms", FAA document FAA-ERAM-2008-0423
8.	"ERAM Flight Data Processing (FDP) and Weather Data Processing (WDP) Algorithms", FAA document FAA-ERAM-2006-0045
9.	"Flightaware – Flight Tracking/Flight Status", <a href="http://flightaware.com">flightaware.com</a>
10.	National Digital Forecast Database GRID2 Decoder, <a href="https://www.weather.govmdl/degrib_home">https://www.weather.govmdl/degrib_home</a>
11.	Python IDE for Eclipse, <a href="http://www.pydev.org">http://www.pydev.org</a>
12.	Git fast version control, <a href="https://git-scm.com">https://git-scm.com</a>
13.	"CUDA By Example", Sanders and Kandrot
14.	"CUDA C Programming Guide", Nvidia Corporation

## Appendix E. List of Abbreviations

ARD	Along Route Distance
ASDI	Aircraft Display for Industry
ATC	Air Traffic Control
BADA	Base of Aircraft Data
CAS	Calibrated Air Speed
CPU	Central Processing Unit

CSV	Comma Separated Values, a file format
FAA	Federal Aviation Administration
FIR	Flight Information Region
GPS	Global Positioning System
GPU	Graphics Processing Unit
GRIB	Grid in Binary
IDE	Integrated Development Environment
ISA	International Standard Atmosphere
NMI	Nautical Miles
NOAA	National Oceanic and Atmospheric Administration
ODE	Ordinary Differential Equation
PSO	Particle Swarm Optimization
ROCD	Rate of Climb or Descent
TAS	True Air Speed
TOD	Top Of Descent
WGS	World Geodetic System